Published in final edited form as:
J Immunol. 2012 November 15; 189(10): 5001–5015. doi:10.4049/jimmunol.1101013.

The B10 *Idd9.3* locus mediates accumulation of functionally superior CD137^{pos} T regulatory cells in the NOD Type 1 diabetes model

Kritika Kachapati[*], **David E. Adams**[*], **Yuehong Wu**[*], **Charles A. Steward**[‡], **Daniel B. Rainbow**[+], **Linda S. Wicker**[+], **Robert S. Mittler**[†], and **William M. Ridgway**[*,§,1]

[*]Division of Immunology, Allergy and Rheumatology, University of Cincinnati College of Medicine

[†]Department of Surgery and Emory Vaccine Center, Atlanta, GA

[‡]The Wellcome Trust Sanger Institute, Wellcome Trust Genome Campus, Hinxton, United Kingdom

[+]Juvenile Diabetes Research Foundation/Wellcome Trust Diabetes and Inflammation Laboratory, Department of Medical Genetics, Cambridge Institute for Medical Research, University of Cambridge, Cambridge CB2 0XY, UK

Abstract

CD137 is a T cell costimulatory molecule encoded by the prime candidate gene (designated *Tnfrsf9*) in NOD.B10 *Idd9.3* congenic mice protected from type one diabetes (T1D). NOD T cells show decreased CD137-mediated T cell signaling compared to NOD.B10 *Idd9.3* T cells, but it has been unclear how this decreased CD137 T cell signaling could mediate susceptibility to T1D. We and others have shown that a subset of T regulatory cells (Tregs) constitutively expresses CD137 (whereas T effectors do not, and only express CD137 briefly after activation). Here we show that the B10 *Idd9.3* region intrinsically contributes to accumulation of CD137^{pos} Tregs with age. NOD.B10 *Idd9.3* mice showed significantly increased percentages and numbers of CD137^{pos} peripheral Tregs compared to NOD mice. Moreover, Tregs expressing the B10 *Idd9.3* region preferentially accumulated in mixed bone marrow chimeric mice reconstituted with allotypically marked NOD and NOD.B10 *Idd9.3* bone marrow. We demonstrate a possible significance of increased numbers of CD137^{pos} Tregs by showing functional superiority of FACS purified CD137^{pos} Tregs *in vitro* compared to CD137^{neg} Tregs in T cell suppression assays. Increased functional suppression was also associated with increased production of the alternatively spliced CD137 isoform, soluble CD137, which has been shown to suppress T cell proliferation. We show for the first time that CD137^{pos} Tregs are the primary cellular source of soluble CD137. NOD.B10 *Idd9.3* mice showed significantly increased serum soluble CD137 compared to NOD mice with age, consistent with their increased numbers of CD137^{pos} Tregs with age. These studies

[§]Corresponding author, HPB room 356, 231 Albert Sabin Drive, University of Cincinnati College of Medicine, Cincinnati, Ohio, 45267-0563 phone: (513) 558 5551 fax: (513) 558 3799.

[1]This work was funded by NIH U19AI56374 (Autoimmunity Centers of Excellence), ADA 1-11-BS-131 (American Diabetes Association), and Award Number I01BX007080 from the Biomedical Laboratory Research & Development Service of the VA Office of Research and Development (**W.M.R.**) and by a joint grant from the Juvenile Diabetes Research Foundation (JDRF) and the Wellcome Trust (LSW). Cambridge Institute for Medical Research (CIMR) is in receipt of a Wellcome Trust Strategic Award (079895) (**L.S.W.**). The resequencing of *Idd9.3* in the NOD mouse strain was performed at the Wellcome Trust Sanger Institute and was funded by Immune Tolerance Network Contract AI 15416, which was sponsored by the National Institute of Allergy and Infectious Diseases, the National Institute of Diabetes and Digestive and Kidney Diseases, and Juvenile Diabetes Research Foundation International. The availability of NOD congenic mice through the Taconic Emerging Models Program has been supported by grants from the Merck Genome Research Institute, the National Institute of Allergy and Infectious Diseases, and the Juvenile Diabetes Research Foundation International.

demonstrate the importance of CD137^{pos} Tregs in T1D and offer a new hypothesis for how the NOD *Idd9.3* region could act to increase T1D susceptibility.

Introduction

Type I diabetes (T1D) is a polygenic autoimmune disease, and several genetic elements implicated in T1D pathogenesis mediate their effects through disruption of immune tolerance (1). In the Non Obese Diabetic (NOD) mouse model of T1D, CD4^{pos}CD25^{pos}Foxp3^{pos} regulatory T cells are unable to control immune destruction of the beta cells in the pancreatic islets during progression to diabetes. NOD.B10 *Idd9.3* congenic mice (that have been shown by congenic mapping to have a 1.2 Mb B10 *Idd9.3* region within a larger 5.5 Mb B10 region on chromosome four) have a 40% reduced incidence of diabetes compared to NOD mice (2, 3). The *Idd9.3* region encodes 15 known genes including *Tnfrsf9*, which is the strongest candidate gene in the region. *Tnfrsf9* encodes the CD137 protein and there are three coding variants between the NOD and B10 *Tnfrsf9* gene, two non-synonymous SNPs and an alanine insertion in NOD (2). CD137 is an inducible T cell co-stimulatory molecule and a member of the TNF receptor superfamily (4). T cells with the B10 *Tnfrsf9* allele have enhanced proliferation and IL-2 production when stimulated via CD137 compared to NOD T cells (2). We and others have shown that CD137 is constitutively expressed by a subset of CD4^{pos}CD25^{pos} T regulatory cells, but not by non-Treg CD4^{pos} T cells (5–9). Marson et al., in particular, showed that *Tnfrsf9* is one of a small set of genes directly upregulated by Foxp3 (10). The Mathis group, moreover, showed that Tregs isolated specifically from NOD pancreatic islets upregulated *Tnfrsf9* (11). It has also been recently shown that *Idd9.2* and *9.3* protective alleles function in CD4^{pos} T cells to prevent expansion of pathogenic islet-specific CD8+ T cells (12). CD137 signaling promotes proliferation and survival of natural Tregs *in vitro*, which is enhanced by IL-2 (6, 13). We have shown that agonist anti-CD137 antibody prevents diabetes in NOD mice, and increases the number of CD4^{pos}CD25^{pos} T cells *in vivo* (5). Here we show, for the first time, that the B10 *Idd9.3* region mediates enhanced accumulation of peripheral CD137^{pos} Tregs *in vivo*. NOD.B10 *Idd9.3* congenic mice accumulate significantly more CD137^{pos} Tregs with age compared to NOD mice. We show that CD137^{pos} Tregs are functionally superior to CD137^{neg} Tregs in suppressing T cells *in vitro* by both contact dependent and independent suppression. Treg mediated contact independent mechanisms include multiple short-range suppressive factors such as IL-10 (14), TGF-β (15), galectin (16), and IL-35 (17). While contact independent suppression is still not well understood, many papers have now demonstrated contact independent suppression mediated in transwell plate assays (18–29). Alternate splicing produces two isoforms of CD137: full length CD137 that is expressed on the cell membrane and soluble CD137 in which transmembrane exon 8 is spliced out (30). Soluble CD137 is increased in autoimmune diseases such as rheumatoid arthritis, multiple sclerosis and systemic lupus (31, 32). It has been shown that soluble CD137 can inhibit T cell proliferation, and hypothesized that increased soluble CD137 functions as a negative feedback mechanism to control overactivation of pathogenic cells in autoimmunity (32, 33). We present novel data showing that CD4^{pos}CD25^{pos}CD137^{pos} Tregs are a major cellular source of soluble CD137. We also show that older NOD.B10 *Idd9.3* congenic mice have significantly increased serum soluble CD137 compared to NOD mice. We suggest that the maintenance and long-term accumulation of functionally superior peripheral CD137^{pos} T regulatory cells (as we show in NOD.B10 *Idd9.3* congenic mice protected from T1D), and their production of soluble CD137, may play a critical role in protection from autoimmune diseases such as type one diabetes.

Materials and Methods

Mice and reagents—NOD/MrkTac mice were obtained from Taconic. NOD.B10 *Idd9.3* mice were developed as previously described (2, 3) and are available from The Jackson Laboratory as Stock No. 012311. The NOD.B6-*Ptprc* (hereafter referred to as "NOD.CD45.2"), which has a 1 Mb congenic interval, was developed as previously described (34) and is available from The Jackson Laboratory as Stock No. 014149). NOD.Foxp3-GFP knock-in mice (Hereafter "NOD.Foxp3-GFP mice") were a kind gift from Vijay Kuchroo and Ana Anderson of Harvard University. The mice were generated by crossing the C57BL/6 Foxp3-GFP KI generated in Dr. Kuchroo's laboratory (35) to NOD Mrk/Tac for 12 generations and then intercrossed for hemi/homozygosity for Foxp3-GFP KI mutation. NOD.B10 *Idd9.3* Foxp3-GFP mice were produced by crossing the NOD.B10 *Idd9.3* to NOD.Foxp3-GFP mice, intercrossing and selecting mice positive for both the *Idd9.3* region and the Foxp3-GFP KI mutation. NOD.Foxp3-GFP mice have normal incidence of T1D in our Cincinnati LAMS facility while the NOD.B10 *Idd9.3* Foxp3-GFP mice show protection from T1D similar to NOD.B10 *Idd9.3* mice in our colony. Mice were maintained under specific pathogen-free conditions in our animal facilities. Mice were handled in accordance with the institutional animal care guidelines of University of Pittsburgh School of Medicine and University of Cincinnati School of Medicine. Anti-CD137 monoclonal antibody (clone 3H3) has been previously described (36). Antibodies against mouse 2.5G2-Fc, CD4-APC, CD4-APC-Cy7, CD25-PerCP-Cy5.5, CD25-FITC, Strepavidin-PE and Strepavidin-APC were purchased from BD Biosciences. CD3/CD28 coated beads and recombinant mouse IL-2 were purchased from Invitrogen (California). Primers for mouse Gapdh (4352339E-0801016) and Beta-2 microglobulin (Mm00437762_m1) were purchased from Applied Bioscience (California). We used custom designed primers for membrane bound and soluble CD137 (Applied Bioscience). For membrane bound CD137, the forward primer was CCCCCTGTGGTGAGCTTC and the reverse primer was AGGAGGGCACTCCTTGCA. For soluble CD137, the forward primer was CCCCCTGTGGTGAGCTTC and the reverse primer was GGGAGGACCAGCATTTAAGAAGA. The probe for both the primers is TCCCAGTACCACCATT.

Resequencing the *Idd9.3* interval in the NOD mouse strain and identifying polymorphisms

The resequencing of *Idd9.3* in the NOD mouse strain involved aligning the bacterial artificial chromosome (BAC) clone end sequences of the NOD library against the B6 mouse genome sequence (37). From this, ten NOD BAC clones that formed a minimal sequencing tile path spanning the 1.2 Mb *Idd9.3* interval were selected and sequenced at the Wellcome Trust Sanger Institute and deposited at the European Molecular Biology Laboratory http://www.ebi.ac.uk/embl (clone DN-135J18, accession number CU463327; DN-79L21, CU210939; DN-382D20, CU207373; DN-272K19, CU424443; DN-192H14, CU210934; DN-117C24, CU210933; DN-106G2, CU210932; DN-129I7, CU207371; DN-266N3, CU207342; DN-404A18, CU407306). As all the B6 and B10 SNPs were found to be identical by descent throughout the *Idd9.3* region (Mouse phenome database: http://phenome.jax.org), we identified polymorphisms between NOD and B6 in the *Idd9.3* interval. The NOD BAC clone sequences spanning the *Idd9.3* interval were aligned to the B6 mouse genome sequence (NCBI m37 mouse assembly) by using the sequence search and alignment by hashing algorithm program (38). The polymorphisms were entered into T1DBase (39, 40) and displayed graphically using GBrowse (41) (Supplemental Fig 1). The SNP density plots were generated by counting the number of SNPs in 10-kb windows, sliding 2 kb at a time, and plotting the count at the midpoint of each window (Supplemental Fig 1). The Wellcome Trust Sanger Institute has next generation sequenced 17 mouse strains, including NOD/ShiLtJ (http://www.sanger.ac.uk/resources/mouse/genomes/). The

SNP information was downloaded for the *Idd9.3* region and entered into T1DBase, and can be viewed at www.t1dbase.org.

Flow Cytometry—For absolute cell counts, NOD and NOD.B10 *Idd9.3* splenocytes or thymocytes were extracted and counted using a hemocytometer. For staining membrane bound CD137, the cells were incubated with 2.4G2 Fc block. For FACS analysis, cells were stained with CD4-APC, CD25-FITC and stained for CD137 using IgG2a anti-CD137 or IgG2a isotype control antibody, then stained with anti-IgG2a biotin and strepavidin-PE and analyzed on a FacsCaliber (BD Biosciences). The cells were serially gated for total number of lymphocytes (by Fsc and Ssc), CD4, $CD4^{pos}CD25^{pos}$, $CD4^{pos}CD25^{pos}CD137^{neg}$ and $CD4^{pos}CD25^{pos}CD137^{pos}$ T cells. The percentage staining in each gate was multiplied by the absolute number of cells to calculate the total number of lymphocytes, $CD4^{pos}$, $CD4^{pos}CD25^{pos}$ and $CD4^{pos}CD25^{pos}CD137^{neg}$ and $CD4^{pos}CD25^{pos}CD137^{pos}$ T cells. For intracellular staining, the splenocytes were stained with CD4-APC-Cy7, CD25-Percp-Cy5.5, CD137-PE and fixed with 2% formaldehyde (methanol free) and permeabilized with 0.3% saponin. Intracellular staining was performed with Foxp3-PE or IgG2a isotype-PE (eBioscience), Bclxl-Alexa-Fluor488 or IgG isotype-Alexa-Fluor488 (Cell Signaling), Bcl2-Alexa-Fluor488 or IgG1 isotype-Alexa-Fluor488 (BioLegend) and Ki-67-Alexa-Fluor488 or IgG isotype-Alexa-Fluor488 (Novus Biologicals). Anti-mouse Ki-67 or IgG isotype control antibody was labeled with APEX Alexa-Fluor488 Antibody Labeling Kit (Invitrogen). Foxp3 staining was performed using eBioscience Fixation/Permeabilization Kit. (NOD.CD45.2 X NOD.B10 *Idd9.3*) F1 bone marrow chimera spleen and pancreatic lymph nodes were stained with CD4-APC-Cy7, CD25-Percp-Cy5.5, CD45.1-FITC, CD45.2-APC and CD137-PE or IgG2a isotype-PE and analyzed on a FACSCantos (BD Biosciences). All FACS data was analyzed using FlowJo (Treestar, Oregan).

Bone Marrow Chimera construction—9–13 week old (NOD.CD45.2 X NOD.B10 *Idd9.3*) F1 mice were irradiated with 800–1200 Rads (the dose was varied as we gained experience in this procedure, to optimize depletion of host cells). 15–25 million bone marrow cells from 5–12 week old NOD.B10 *Idd9.3* and NOD.CD45.2 mice were extracted without RBC lysis. Mature CD4, CD8 and CD90 cells were removed using magnetic beads (Miltenyi Biotech, California) and the bone marrow was then mixed at a 1:1 ratio and injected into the irradiated F1 mice. Recipient mice were given water treated with antibiotic (neomycin trisulfate salt hydrate) for two weeks after transfer. The recipient F1 mice were sacrificed 12–20 weeks post injection for analysis of peripheral T cell populations by FACS.

RT-PCR—CD4 T cells were extracted from splenocytes using CD4 magnetic beads (Miltenyi Biotech, California). The CD4 T cells were blocked with 2.4G2 and stained with CD4-APC-Cy7, CD25-FITC, and anti-CD137-APC as above. The cells were sorted using a BD FacsAria machine (BD Bioscience) into $CD4^{pos}CD25^{neg}CD137^{neg}$, $CD4^{pos}CD25^{pos}CD137^{neg}$ and $CD4^{pos}CD25^{pos}CD137^{pos}$ cell subsets, RNA was extracted from the sorted cells using an RNeasy mini kit (Qiagen) and converted into cDNA (Promega Reverse Transcription System). Quantitative Real Time Polymerase Chain Reaction (RT-PCR) was performed on the cDNA using primers for B2m, soluble CD137 and membrane bound CD137 using a StepOnePlus Real-Time PCR system (Applied Biosystems). The CT values of the gene of interest were subtracted from the CT of the housekeeping gene (Gadph or B2m) to produce the delta CT (designated "ΔCT") and the data graphed using GraphPad Prism 5 (Version 5.02).

Proliferation Assay—The $CD4^{pos}CD25^{neg}CD137^{neg}$, $CD4^{pos}CD25^{pos}CD137^{neg}$ and $CD4^{pos}CD25^{pos}CD137^{pos}$ splenocytes were stained and sorted using BDAria (BD Bioscience) with 90–95% purity. 50,000 sorted cells were cultured at 37°C with 5% CO_2

with (a) 25U/ml IL-2 or (b) 25U/ml/IL-2 and 1.25 ug/ml anti-CD3 in triplicate wells. The cells were pulsed with 1 μCi ^{3}H labeled thymidine on day 3 and harvested after 16 hours using a beta scintillation counter. For the suppression assay 50,000 $CD4^{pos}CD25^{neg}CD137^{neg}$ T cells were cultured in U-bottom 96 well plate with 1 ug/well soluble anti-CD3, 50,000 irradiated splenocytes (1500 rads) and varying numbers of $CD4^{pos}CD25^{pos}CD137^{neg}$ or $CD4^{pos}CD25^{pos}CD137^{pos}$ Tregs. All cells were cultured and pulsed with 1 μCi [^{3}H] thymidine on Day 3, 16 hours before harvest. On Day 4, thymidine incorporation was assessed using a beta scintillation counter.

Treg Transwell Suppression Assay—100,000 sorted $CD4^{pos}CD25^{neg}CD137^{neg}$ T cells were cultured with 100,000 irradiated splenocytes (1500 rads) and 1.25 ug/ml soluble anti-CD3 in the bottom wells of a 96 well transwell plate (Corning). 25,000 or 50,000 $CD4^{pos}CD25^{pos}CD137^{neg}$ or $CD4^{pos}CD25^{pos}CD137^{pos}$ Tregs were cultured in the top wells with 100,000 irradiated (1500 rads) splenocytes and 1.25 ug/ml soluble anti-CD3. In some assays the sorted $CD4^{pos}CD25^{pos}CD137^{neg}$ or $CD4^{pos}CD25^{pos}CD137^{pos}$ Tregs were also cultured in the bottom of the transwell along with the $CD4^{pos}CD25^{neg}CD137^{neg}$ T effector cells (with no Tregs in the top transwell) to directly compare contact dependent and independent suppression by the same sorted cells. In some cases, the cells were cultured with 50,000 CD3/CD28-coated beads (Invitrogen) in the absence of APCs. The cells were cultured at 37°C in 5% CO_2 and were pulsed with 1 μCi [^{3}H] thymidine on Day 3. The cells in the bottom wells were harvested and counted using a beta scintillation counter.

ELISA—Mouse 4-1BB DuoSet Elisa system (R&D Systems, California) was used to detect soluble CD137 from serum and culture supernatants. The kit uses rat anti-mouse 4-1BB capture antibody and biotinylated goat anti-mouse 4-1BB detection antibody. Recombinant mouse 4-1BB, provided in the kit, was used as a standard. DeltaSoft software was used to calculate the amount of soluble CD137 in each well based on the standard for each experiment.

Treg culture—50,000 $CD4^{pos}CD25^{pos}CD137^{neg}$ or $CD4^{pos}CD25^{pos}CD137^{pos}$ Tregs were cultured in 96 well U-bottom plate with no IL-2 (unstimulated), 25U/ml mouse recombinant IL-2 alone with or without 1.25 ug/ml of anti-CD3 antibody for 4 days, and the supernatants were tested for soluble CD137 as above by ELISA.

Data analysis

All statistical analysis was performed using either the unpaired T test or the Mann-Whitney test in GraphPad Prism 5 (Version 5.02).

Results

Increased accumulation of $CD137^{pos}$ Tregs with the B10 versus the NOD *Idd9.3* region *in vivo*

We previously demonstrated that agonist anti-CD137 treatment prevents diabetes in NOD mice, that a subset of Tregs constitutively expresses CD137, and that anti-CD137 binds to $CD4^{pos}CD25^{pos}CD137^{pos}$ Tregs *in vitro* and *in vivo* (5). Our results suggested that $CD137^{pos}$ Tregs may be important in T1D pathogenesis. We quantified CD137 expression on $CD4^{pos}CD25^{pos}$ T cells as previously published (5) and as in Fig 1a, which shows a well-defined $CD137^{pos}$ population compared to isotype control; $CD137^{pos}$ cells constitute 30% of all $CD4^{pos}CD25^{pos}$ T cells in the representative example shown. Since it has been previously shown that CD137 promotes CD4 and CD8 T cell survival (4, 42, 43), we investigated changes in the frequency and the number of $CD137^{pos}$ T regulatory cells with age in non-diabetic NOD and NOD.B10 *Idd9.3* congenic mice. The percentage of $CD137^{pos}$

cells within the $CD4^{pos}CD25^{pos}$ T cell population significantly declines with age in NOD, but not in NOD.B10 *Idd9.3* spleen (P=0.006, Fig 1b). At both younger (3–9 weeks) and older (21–36 week) ages, the percentage of splenic CD137-expressing Tregs are significantly higher in NOD.B10 *Idd9.3* mice than in NOD mice (P=0.01 and P<0.0001 Fig 1b). The absolute number of $CD137^{pos}$ Tregs significantly increased with age from 3–9 weeks to 21–36 weeks in NOD.B10 *Idd9.3* congenic mice (P=0.03, Fig 1c). In addition there was a significant increase in the absolute number of $CD137^{pos}$ splenic Tregs in older NOD.B10 *Idd9.3* congenic mice compared to age matched NOD mice (P=0.03, Fig 1c). However the number of NOD $CD137^{pos}$ Tregs did not change with age despite an age related decline in the percentage NOD $CD137^{pos}$ Tregs. (We also looked at the percentage of $CD137^{pos}$ Tregs at 10–20 weeks of age and observed no significant differences compared the other age groups of either strain - data not shown). Consistent with previously published observations (44), the number of splenic $CD4^{pos}CD25^{pos}$ T cells increased significantly with age in both strains with no difference between the strains (Supp Fig 2a). This explains the lack of decline of $CD137^{pos}$ Treg number in NOD with age despite a significant drop in the percent of $CD137^{pos}$ Tregs. Similarly, it also explains the significant increase in the total number of $CD137^{pos}$ Tregs with age in NOD.B10 *Idd9.3* mice (P=0.03, Fig 1c), despite the finding that the percentage of $CD137^{pos}$ Tregs did not increase with age (Fig 1b). Thus the increased number of NOD.B10 *Idd9.3* $CD4^{pos}CD25^{pos}CD137^{pos}$ T cells with age is due to a combination of an increased percentage of $CD137^{pos}$ T cells and an increased absolute number of $CD4^{pos}CD25^{pos}$ T cells in older NOD.B10 *Idd9.3* mice. There was also no difference in the percentage of $CD4^{pos}CD25^{pos}$ T cells with age in either strain (Supp Fig 2b). Both NOD and NOD.B10 *Idd9.3* congenic mice showed significant increases in $CD4^{pos}$ T cells and total numbers of splenic lymphocytes with age (Supp Fig 2 c, d), but there was no difference between NOD.B10 *Idd9.3* and NOD mice in the corresponding age groups.

We next studied the percentages and total number of thymic $CD137^{pos}$ Tregs in NOD and NOD.B10 *Idd9.3* congenic mice and found that they were consistent with the peripheral population results. The percentage and absolute number of thymic $CD137^{pos}$ Tregs was significantly higher in 21–36 week old NOD.B10 *Idd9.3* versus NOD mice (P=0.002, Supp Fig 3a and P=0.02, Supp Fig 3b). The total number of thymic $CD4^{pos}CD25^{pos}$ T cells, however, remained approximately constant with age in both strains (Supp Fig 3c). The percentage of NOD.B10 *Idd9.3* $CD4^{pos}CD25^{pos}$ thymocytes rose significantly (P=0.02, Supp Fig 3d). The number of $CD4^{pos}$ thymocytes significantly declined with age in both strains with no difference between the two strains (Supp Fig 3e). The total number of thymocytes significantly decreased with age in NOD (P=0.007, Supp Fig 3f); it decreased, but not significantly, in older NOD.B10 *Idd9.3* mice. In summary, it is clear that the decreased number of NOD thymic $CD137^{pos}$ Tregs with age was due to a decreased percentage of these cells; in older NOD.B10 *Idd9.3* mice a significant increase in the percentage of $CD137^{pos}$ Tregs caused a significant increase in the number of thymic $CD137^{pos}$ Tregs.

In order to begin to understand possible reasons for increased NOD.B10 *Idd9.3* $CD137^{pos}$ Treg accumulation with age we examined the per cell surface expression of CD137 at the same time points. The mean florescence intensity of CD137 on $CD4^{pos}CD25^{pos}CD137^{pos}$ T cells was significantly greater in young (3–9 week old) NOD.B10 *Idd9.3* versus age matched NOD (P=0.009, Fig 1d). Although the percentage of $CD4^{pos}CD25^{pos}CD137^{pos}$ T cells declined markedly in 21–36 week old NOD spleen (P= 0.006, Fig 1b), the $CD137^{pos}$ Tregs found in old NOD spleen expressed a significantly higher level of CD137 per cell compared to young NOD splenic Tregs (P=0.003, Fig 1d); not significantly different from old NOD.B10 *Idd9.3* cells (Fig 1d). Similar CD137 MFI was found in thymic $CD4^{pos}CD25^{pos}CD137^{pos}$ T cells with age—old thymic NOD $CD137^{pos}$ Tregs expressed more CD137 per cell than young NOD cells (P=0.0004, Supp Fig 3g) and young thymic

NOD.B10 *Idd9.3* CD137^{pos} Tregs were significantly higher than on young NOD cells (P=0.0003, Supp Fig 3g). These findings suggest that early, increased expression of CD137 on Tregs might enhance long term accumulation of those cells, consistent with the previously published role of CD137 on CD8 and CD4 T cell survival *in vivo* and *in vitro* (42, 43, 45). The increased expression of CD137 on a per cell basis in young NOD.B10 *Idd9.3* congenic spleen is associated with the increase in the number of CD4^{pos}CD25^{pos}CD137^{pos} T cells with age. Overall, these studies show that the B10 *Idd9.3* region enhances accumulation of CD137^{pos} Tregs in the NOD.B10 *Idd9.3* congenic mice, and supports the hypothesis that CD137 is important for the long-term accumulation of CD137^{pos} Tregs.

The above results depended on identifying Tregs by CD25 expression. While this is a recognized Treg marker, it can also be a marker of T cell activation, as can CD137. It was important to evaluate the peripheral Treg subsets by intracellular Foxp3 expression to ensure that the increased number of NOD.B10 *Idd9.3* CD4^{pos}CD25^{pos}CD137^{pos} T cells with age were truly Tregs. To evaluate this, we first performed intracellular Foxp3 staining at all age points. We showed that the overwhelming majority of CD4^{pos}CD25^{pos}CD137^{pos} T cellsare Foxp3 positive (Fig 2a, b) and that there is no significant difference in percentage of Foxp3 positive cells between CD4^{pos}CD25^{pos}CD137^{neg} and CD4^{pos}CD25^{pos}CD137^{pos} T cells in either 5–9 week old or 20–30 week old NOD or NOD.B10 *Idd9.3* congenic mice (Fig 2a, b). Our results match a previous study that showed similar percent Foxp3 expression in CD4^{pos}CD25^{pos} T cells in NOD with age (46), and shows that the increased number of NOD.B10 *Idd9.3* CD4^{pos}CD25^{pos}CD137^{pos} T cells is not due to an expansion of non-Tregs in this subset. We also found a slight increase in isotype staining with age (not shown), and since we subtracted the isotype staining (see Figure 2c for a representative example for gating) to calculate “true positive” Foxp3 cells, we may have underestimated the true Foxp3 expression (representative FACS plots for Foxp3 vs. CD137 (Figure 2d) and CD4 vs. Foxp3 (Figure 2e) for NOD and NOD. B10 *Idd9.3* are also shown). After all the studies in this paper were performed, we obtained NOD.Foxp3-GFP mice, and used these mice to create NOD.B10 *Idd9.3* Foxp3-GFP mice. We aged these mice and used them to evaluate the percent of Foxp3-GFP positive cells in the CD4^{pos}CD25^{pos}CD137^{neg} and CD4^{pos}CD25^{pos}CD137^{pos} subsets in NOD and NOD.B10 *Idd9.3* at the same time points as we examined above (Fig 2a, b). The results (Figure 3) support the conclusions of Figures two above and show that well over 90% of CD4^{pos}CD25^{pos}CD137^{neg} and CD4^{pos}CD25^{pos}CD137^{pos} subsets in NOD and NOD.B10 *Idd9.3,* both young and old, were Foxp3-GFP positive, and that there were no significant differences between the strains (Figures 3a, b show the pooled result while Figure 3c shows representative FACS plots in NOD.Foxp3-GFP and NOD.B10 *Idd9.3* Foxp3-GFP mice). The combined results of Figures two and three very strongly show that the increase of CD4^{pos}CD25^{pos}CD137^{pos} cells in NOD.B10 *Idd9.3* mice with age truly represents a significant increase in Foxp3 expressing CD137^{pos} Tregs.

Increased accumulation of CD137^{pos} Tregs with the B10 versus the NOD *Idd9.3* region in mixed bone marrow chimeras *in vivo*

The finding of increased CD137^{pos} Tregs in NOD.B10 *Idd9.3* compared to NOD mice with age probably reflects multiple biological processes and complex intrinsic/extrinsic cellular effects in separate animals/strains. In order to confirm the finding of increased accumulation of Tregs expressing the B10 *Idd9.3* region, we sought to demonstrate increased accumulation of these cells compared to cells with the NOD *Idd9.3* region, in the same animal. To do this, and to test whether the B10 *Idd9.3* region intrinsically mediated increased accumulation of CD137^{pos} Tregs, we constructed mixed bone marrow chimeras using NOD and NOD.B10 *Idd9.3* CD137^{pos} bone marrow transferred into irradiated

(NOD.CD45.2 x NOD.B10 *Idd9.3* (CD45.1)) F1 mice. The resulting chimeric mice were analyzed for effective reconstitution and relative ratios of allotypically marked cells as shown in Figure 4a. In the mixed bone marrow chimera mice, the percentage of peripheral (splenic or pancreatic lymph node) $CD4^{pos}CD25^{pos}CD137^{pos}$ T cells expressing the B10 CD137 allotype was significantly increased compared to the NOD allotype (Fig 4b, c). $CD4^{pos}CD25^{pos}CD137^{neg}$ Tregs from the same individual mice, in contrast, showed no significant CD45.1 vs. CD45.2 population differences (Fig 4a–c). Since the percentage of B10 and NOD allotype were from the $CD137^{pos}$ Treg population in the same bone marrow chimeric mouse, the total number of splenocytes or lymph node cells were the same for each cell population; hence the total numbers of B10 or NOD allotype $CD137^{pos}$ Tregs in the bone marrow chimeric mice were exactly proportional with these percentages. There was statistically no significant difference in thymic CD45.1 vs. CD45.2 proportions in $CD4^{pos}CD25^{pos}CD137^{neg}$ and $CD4^{pos}CD25^{pos}CD137^{pos}$ T cell populations (data not shown). These results, which are entirely consistent with the studies in Figure one, strongly support the hypothesis that the B10 CD137 region intrinsically and selectively mediates enhanced accumulation of $CD137^{pos}$ Tregs in the periphery.

Enhanced proliferation of $CD137^{pos}$ Tregs *ex vivo* and *in vitro* but no significant difference between NOD and NOD.B10 Idd9.3 congenic mice

CD137 co-stimulation causes proliferation of Tregs *in vitro* (13, 36) and *in vivo* (47). The increased frequency and accumulation of $CD137^{pos}$ Tregs in NOD.B10 *Idd9.3* congenic mice could be due to intrinsic factors, such as greater proliferative capacity or enhanced cell survival mediated by the B10 CD137 allotype. To test proliferative capacity, we cultured NOD and NOD.B10 *Idd9.3* $CD137^{pos}$ and $CD137^{neg}$ Tregs in the presence of IL-2 (Fig 5a) or IL-2 and CD3 (Fig 5b) or with no IL2 (unstimulated) (Supp Fig 4c). The proliferation of $CD137^{pos}$ Tregs was significantly greater than $CD137^{neg}$ Tregs under both culture conditions and in both strains, but there was no difference in proliferation of $CD137^{pos}$ Tregs between NOD and NOD.B10 *Idd9.3* mice (Fig 5a, b). As expected, Tregs cultured with no IL-2 showed virtually no proliferation (Supp Fig 4c). Next, we quantified expression of the nuclear protein Ki-67, as a marker for proliferation *ex vivo*. Consistent with the *in vitro* results, a significantly higher percentage of $CD137^{pos}$ Tregs were Ki-67 positive *ex vivo* compared to $CD137^{neg}$ Tregs in both NOD and NOD.B10 *Idd9.3* mice (Fig 5c). Again, we found no difference in percentage of Ki-67 positive $CD137^{pos}$ Tregs between NOD and NOD.B10 *Idd9.3* mice. These studies suggest that the increased numbers and frequency of $CD137^{pos}$ Tregs in NOD.B10 *Idd9.3* congenic mice with age could not be explained by enhanced proliferation mediated by the B10 allotype.

Viability studies in CD137 stimulated and unstimulated T cells have shown that CD137 signaling prevents activation induced cell death (AICD) by repressing DNA fragmentation (48). Since CD137 signaling can upregulate the pro-survival molecule Bcl-xL(42), we tested the expression of Bcl-xL in NOD and NOD.B10 *Idd9.3* Treg subsets. We found significantly increased Bcl-xL mRNA expression in NOD.B10 *Idd9.3* versus NOD $CD137^{pos}$ Tregs (P=0.04, Fig 6a). We also found increased expression of Bcl-xL in NOD.B10 *Idd*9.3 versus NOD $CD137^{neg}$ Tregs (P= 0.008), which suggests CD137 is not necessary for upregulation of Bcl-xL in these NOD.B10 *Idd*9.3 cells. We next tested Bcl-xL mRNA expression in the mixed bone marrow chimera cell subsets, stratified by allotype. In the mixed bone marrow chimera experiments, $CD137^{pos}$, but not $CD137^{neg}$ Tregs with the B10 allotype expressed significantly increased Bcl-xL (P=0.008, Fig 6b). As a control, we tested levels of Bcl-2, a pro-survival molecule not known to be associated with CD137 signaling. There were no significant differences in expression of Bcl2 in NOD vs. NOD.B10 *Idd9.3* $CD137^{pos}$ or $CD137^{neg}$ Tregs, in contrast to Bcl-xL (Fig 6c). In the mixed bone marrow chimeric mice, the $CD137^{pos}$ but not the $CD137^{neg}$ Treg subset showed

significantly increased Bcl2 mRNA in B10 allotype vs. NOD allotype cells (p=0.0003, Fig 6d). To summarize, the CD137^{pos} Treg subsets (in both normal NOD.B10 *Idd9.3* mice and in the B10 allotype cells of bone marrow chimera mice) showed significant increases of Bcl-xL mRNA. However in CD137^{neg} Tregs, NOD.B10 *Idd9.3* Tregs also show increased Bcl-xL mRNA compared to NOD, and B10 allotype CD137^{pos} Tregs in the bone marrow chimeras also showed upregulated Bcl2 message. To understand the significance of these findings, we examined protein levels of these survival molecules in both NOD and NOD.B10 *Idd9.3* Treg subsets. Contrary to the PCR results, the Bcl-xL expression per cell did not vary between the NOD.B10 *Idd9.3* versus NOD CD137^{pos} Tregs (Fig 6e). Similarly, CD137^{pos} Tregs showed no difference in Bcl2 MFI in between NOD.B10 *Idd9.3* and NOD (Fig 6f). The greater accumulation of NOD.B10 *Idd9.3* CD137^{pos} Tregs compared to NOD could be due to enhanced survival of cells expressing the B10 CD137 allele. We tested this *in vitro* by culturing NOD and NOD.B10 *Idd9.3* Tregs subsets in the presence of IL-2 or IL-2/CD3 as above. Under both conditions, the percentage of live, early apoptotic (Annexin positive), late apoptotic (Annexin/PI double positive) or dead (PI positive) cells did not differ between NOD and NOD.B10 *Idd9.3* in both CD137^{neg} or CD137^{pos} Tregs (data not shown). Therefore while the increased expression of Bcl-xL mRNA in Tregs expressing the B10 CD137 allele is intriguing, it is not definitive. In addition, since we have no evidence of increased survival *in vitro*, we cannot confirm or exclude the possibility that expression of the B10 CD137 allele causes survival advantage of Tregs without further studies.

Functionally superior contact-dependent and contact-independent suppression mediated by CD137^{pos} vs. CD137^{neg} Tregs

Our results show enhanced accumulation of CD137^{pos} Tregs in NOD.B10 *Idd9.3* mice. To understand the possible significance of increased percentages and numbers of CD137^{pos} Tregs with age, we investigated functional differences between CD137^{neg} and CD137^{pos} Treg subsets. We performed an *in vitro* Treg contact dependent suppression assay using NOD CD4^{pos}CD25^{neg}CD137^{neg} T effector cells and titrated numbers of syngeneic NOD CD137^{pos} or CD137^{neg} Tregs (Fig 7a). CD137^{pos} Tregs were significantly functionally superior to CD137^{neg} Tregs at every ratio (through 1:32, P=0.002) of Treg:T effector tested (Fig 7a). Next, we tested NOD.B10 *Idd9.3* Treg subsets in the same assay system and again found that NOD.B10 *Idd9.3* CD137^{pos} Tregs were functionally superior to CD137^{neg} Tregs when suppressing NOD.B10 *Idd9.3* CD4^{pos}CD25^{neg}CD137^{neg} T effector cells (Fig 7b); however the amount of suppression by NOD.B10 *Idd9.3* CD137^{pos} Tregs was very comparable to NOD CD137^{pos} Tregs (Fig 7b vs. 7a). We directly compared the suppressive capacity of NOD and NOD.B10 *Idd9.3* CD137^{pos} Tregs, in the same experiment, against NOD CD4^{pos}CD25^{neg}CD137^{neg} T effector cells and found no significant difference in the suppressive capacity of the CD137^{pos} Tregs of these two strains (Fig 7c).

Next we tested whether CD137^{pos} Tregs can mediate suppression in a contact-independent manner. Using transwell plates, we cultured CD4^{pos}CD25^{neg}CD137^{neg} T cells in the bottom well and Treg subsets in the upper well; both wells had irradiated splenocytes and anti-CD3 antibodies. At a 1:2 ratio, both CD137^{pos} and CD137^{neg} Tregs significantly suppressed the proliferation of T cells in a contact independent manner, but CD137^{pos} Tregs were significantly more suppressive than CD137^{neg} Tregs (P=0.008, Fig 8a). Next, we directly compared Tregs from the same donor in both contact dependent suppression (Tregs in the bottom well in contact with T effectors) and contact independent suppression (Tregs in the top well). Tregs were significantly more suppressive in the contact dependent assay than in the contact independent assay (Figure 8a, P=0.009 for CD137^{neg} Tregs and P=0.001 for CD137^{pos} Tregs). However, in both assays the CD137^{pos} subset mediated significantly more suppression than the CD137^{neg} subset.

Finally, we assessed contact independent suppression via serial dilution assays. Ratios of Treg to effector below 1:2 did not show a significant difference in suppression between the CD137^{pos} vs. CD137^{neg} Tregs, consistent with a dilutional effect on a soluble factor (Fig 8b). These results suggest that in a contact independent system, both Treg subsets produce soluble suppressive factors when activated, but that CD137^{pos} Tregs can produce either quantitatively higher or different soluble factors that contribute to their functional superiority to CD137^{neg} Tregs.

CD137^{pos} Tregs are the major cellular source of alternately spliced soluble CD137 protein

Alternate splicing produces two isoforms of CD137: full length CD137 expressed on the cell membrane and soluble CD137 in which transmembrane exon 8 is spliced out (30). Previously, however, production of soluble CD137 by Tregs has not been studied. We designed RT-PCR primers (see Methods) that discriminate soluble versus membrane bound CD137 and used them to detect soluble CD137 versus membrane bound CD137 from freshly sorted NOD and NOD.B10 *Idd9.3* subsets. CD137^{pos} Tregs expressed significantly higher levels of soluble and membrane CD137 mRNA compared to CD137^{neg} Tregs in NOD and NOD.B10 *Idd9.3* mice (Fig 9a, b); CD4^{pos}CD25^{neg}CD137^{neg} T cells produced negligible amounts of both isoforms of CD137 mRNA *ex vivo* (Fig 9a, b). Next we sorted the CD137^{pos} and CD137^{neg} Tregs from NOD and NOD.B10 *Idd9.3* mice and cultured them (with IL-2 alone, to promote survival *in vitro* under non-activating conditions) to assess CD137 protein production. The cultured CD137^{pos} Tregs (from either NOD and NOD.B10 *Idd9.3* mice) produced significantly higher levels of soluble CD137 protein compared to CD137^{neg} Tregs; CD4 non-Treg cells did not produce significant amounts of soluble CD137 protein (Fig 9c). There was no significant difference in soluble CD137 protein production between NOD and NOD.B10 *Idd9.3* CD137^{pos} Tregs (Fig 9c, d). We did not detect significant soluble CD137 production from any cell subset in the absence of IL-2 (Supp Fig 4c and data not shown). We have thus established, for the first time, that CD137^{pos} Tregs are the primary T cell source of soluble CD137.

Given that activated T cells express CD137, it was possible that our CD137^{neg} Tregs start producing soluble CD137 under activating conditions. To test this, we cultured CD137^{pos} and CD137^{neg} Tregs from NOD and NOD.B10 *Idd9.3* mice with IL-2 and anti-CD3, and tested culture supernatants on day 4 for soluble CD137. Under these activating conditions, CD137^{neg} Tregs produced some soluble CD137, although still significantly less than CD137^{pos} Tregs in both strains (Fig 9d). Again there was no significant difference in soluble CD137 production between the two strains. These results suggest that Treg activation causes CD137^{neg} Tregs to increase alternate splicing of *Tnfrsf9* with subsequent production of soluble CD137 protein, although still significantly less than CD137^{pos} Tregs. Notably, non-Treg CD4^{pos} cells still did not produce significant amounts of soluble CD137 after stimulation under these activating conditions (Fig 9d). We also tested CD137 membrane expression in CD137^{pos} and CD137^{neg} Tregs from both strains upon IL-2 and CD3 stimulation as above. As expected, the cells sorted as CD137^{neg} Tregs did not express any CD137 pre-culture (Supp Fig 4a). However after IL-2 and CD3 stimulation for 3 days, CD137^{neg} Tregs from both strains showed increased CD137 expression on a per cell basis, but the expression was still much lower than CD137^{pos} Tregs (Supp Fig 4b). Our data suggest that upon *in vitro* IL-2 and CD3 stimulation, CD137^{neg} Tregs start expressing membrane and soluble CD137 but the expression level is still much lower than Tregs that originally express CD137 pre-culture. Next we tested if soluble CD137 is produced by NOD Tregs during *in vitro* suppression in the presence of CD4 T cells and CD3/CD28 beads, in the absence of APCs. Under these conditions, CD137^{neg} Tregs produced soluble CD137 protein but still significantly less (P=0.0001) than CD137^{pos} Tregs (Fig 9e). CD4 T cells cultured with CD3/CD28 beads (rather than irradiated APCs) also produced some soluble

CD137 but significantly less than CD137^{neg} Tregs (P<0.0001). Our findings show that Tregs are the primary source of soluble CD137 *in vitro*. Our results also show that depending on *in vitro* culture conditions CD137^{neg} Tregs can produce some soluble CD137 but significantly less than CD137^{pos} Tregs.

Increased serum soluble CD137 in older NOD.B10 *Idd9.3* mice

We have shown that NOD.B10 *Idd9.3* mice accumulate significantly increased numbers of CD137^{pos} Tregs with age (Fig 1c). We have also shown that CD137^{pos} Tregs are more suppressive (Fig 7a, b) and express more soluble CD137 than CD137^{neg} Tregs (Fig 9a–d). However, NOD and NOD.B10 *Idd9.3* CD137^{pos} Tregs do not differ in either direct contact mediated suppression (Fig 7c) or soluble CD137 production on a per cell basis (Fig 9a–d). We hypothesized that the increased numbers of CD137^{pos} Tregs with age in NOD.B10 *Idd9.3* mice might be reflected in increased soluble CD137 serum levels *in vivo*. In fact old NOD.B10 *Idd9.3* mice had significantly greater amount of serum soluble CD137 levels than age matched NOD mice (Fig 9f). This result shows that the immunological effect of the B10 CD137 allotype could be quantitative, mediated by altering the accumulation of the affected cell subset (i.e., CD137^{pos} Tregs). Increased numbers of Tregs expressing the B10 allele thereby produce increased total amounts of soluble CD137 and also quantitatively expand the overall available contact mediated suppression.

In summary we have established that CD137^{pos} Tregs are a functionally superior Treg subset characterized by surface expression of CD137, superior suppression and production of soluble CD137. Tregs expressing the B10 *Idd9.3* region, compared to the NOD allotype, show increased peripheral accumulation of the functionally superior CD137^{pos} Tregs with age. NOD.B10 *Idd9.3* mice show a correlation between accumulation of CD137^{pos} Tregs with age and increased serum soluble CD137. The data presented here strongly support a critical role for CD137^{pos} Tregs in the regulation of T1D.

Discussion

Our previous studies showed that anti-CD137 antibody treatment increased the number of CD4^{pos}CD25^{pos} T cells in NOD mice and that anti-CD137 antibodies bound specifically to CD4^{pos}CD25^{pos}CD137^{pos} Tregs *in vivo* while preventing diabetes (5). The B10 *Tnfrsf9* allele differs from the NOD allele by three coding variants (2, 3). These sequence polymorphisms differences are likely responsible for the previously described decreased T cell signaling by the NOD allele when stimulated through CD137 (2), and it is known that CD137 signaling enhances Bcl-xL production and mediates cell survival (42). It remained unclear how the decreased NOD allotype CD137 signaling could mediate increased T1D susceptibility (2). We hypothesized that decreased signaling through the NOD CD137 allele, or increased signaling through the B10 CD137 allele, could influence T1D incidence by affecting Treg accumulation, and investigated this hypothesis using NOD and NOD.B10 *Idd9.3* mice. We found increased accumulation of Tregs expressing the B10 *Idd9.3* locus in two separate systems, i.e. *ex vivo* in NOD vs. NOD.B10 *Idd9.3* mice and in a mixed bone marrow chimera system. The absolute number of splenic lymphocytes, CD4 cells and CD4^{pos}CD25^{pos} T cells increased with age in both NOD and NOD.B10 *Idd9.3* mice; however the number of CD4^{pos}CD25^{pos}CD137^{pos} Tregs increased only in NOD.B10 *Idd9.3* mice, reflecting a specific increase in their percentage in NOD.B10 *Idd9.3* and a decreased percentage in NOD. Conversely, in the thymus, the number of CD4^{pos}CD25^{pos}CD137^{pos} T cells decreased in NOD and increased in older NOD.B10 *Idd9.3* mice, reflecting a significantly increased percentage of thymic CD137^{pos} Tregs in older NOD.B10 *Idd9.3* mice. Our data suggests that increased thymic output of CD4^{pos}CD25^{pos}CD137^{pos} T cells in older NOD.B10 *Idd9.3* mice could contribute to the increased accumulation of these cells in the periphery. However we have not conclusively proven increased thymic output, and there

could be additional mechanisms for peripheral accumulation of $CD4^{pos}CD25^{pos}CD137^{pos}$ Tregs. Our data on cell numbers in spleen and thymus of NOD vs. NOD.B10 *Idd9.3* suggests a specific increase in $CD137^{pos}$ Tregs in the NOD.B10 *Idd9.3* mice, but these results could be influenced by many intrinsic and extrinsic causes. To address this point and to show in a separate system that the B10 *Idd9.3* region supported increased accumulation of $CD137^{pos}$ Tregs, we used a mixed bone marrow chimera approach, in which NOD and B10 *Idd9.3*-expressing Tregs could develop in the same mouse and hence have the same extrinsic cellular environment. The studies in bone marrow chimeras show that the increased accumulation of B10 *Idd9.3* expressing Tregs is a cell intrinsic feature in $CD137^{pos}$ Tregs. This does not exclude the possibility that extrinsic factors, particularly IL-2 production from T cells, could also be contributing to expansion or survival of various cell types and protection from diabetes in NOD.B10 *Idd9.3* mice. Given that the B10 allele mediates enhanced IL-2 production in NOD.B10 *Idd9.3* $CD4^{pos}$ T cells (2), this is a likely contributing factor that makes the system more complex and multifactorial.

We also explored possible mechanisms for accumulation of $CD137^{pos}$ Tregs in old NOD.B10 *Idd9.3* mice. First we observed that the NOD.B10 *Idd9.3* $CD137^{pos}$ Tregs do not proliferate more *in vitro* or *in vivo* than the same cell subset in NOD mice, suggesting that proliferation does not account for increased accumulation of $CD137^{pos}$ Tregs in NOD.B10 *Idd9.3* mice. Next, we showed that increased $CD137^{pos}$ Treg accumulation is correlated with increased $CD137^{pos}$ Treg Bcl-xL mRNA expression in both NOD.B10 *Idd9.3* mice and in the $CD137^{pos}$ Tregs with the B10 allotype in the mixed bone marrow chimera mice. The lack of increased Bcl-xL protein expression and the increased Bcl-xL in $CD137^{neg}$ Tregs in NOD.B10 *Idd9.3* mice, however, makes this correlation hard to interpret. Furthermore, we did not see any difference in cell death between NOD and NOD.B10 *Idd9.3* Treg subsets upon *in-vitro* stimulation. Hence further studies need to be performed to establish the mechanism of accumulation of $CD137^{pos}$ Tregs in old NOD.B10 *Idd9.3* mice.

It has been reported that $Foxp3^{pos}$TGF-β^{pos} T cells significantly decline with age in NOD mice and that the aged $CD4^{pos}CD25^{pos}$ T cells are less suppressive against aged $CD4^{pos}CD25^{neg}$ T cells (44, 49). In addition, the increased protection from diabetes in the NOD BDC2.5 model is also associated with increased Foxp3+ T cells with age (50). Therefore it is possible that the increased number of $CD137^{pos}$ Tregs in NOD.B10 *Idd9.3* mice with age could result in increased peripheral immune regulation that could regulate the onset of T1D. We observed that the amount of CD137 (MFI) on the cell surface of $CD4^{pos}CD25^{pos}CD137^{pos}$ Tregs is not decreased on aged NOD $CD137^{pos}$ Tregs—the accumulating $CD137^{pos}$ Tregs on aged NOD are all CD137-high expressers. The CD137 MFI is also higher in young NOD.B10 *Idd9.3* compared to young NOD $CD137^{pos}$ Tregs. The decrease in cellular CD137 expression in young NOD vs. NOD.B10 *Idd9.3* $CD137^{pos}$ Tregs might affect the accumulation of total number of surviving cells long term. Increased expression of an allele that in itself mediates increased signaling could combine to produce an intrinsically mediated signal that results in accumulation of these $CD137^{pos}$ Tregs in NOD.B10 *Idd9.3* mice. This is entirely consistent with studies of the function of CD137 in CD137 knockout mice, which have decreased long term survival of antigen specific CD8 T cells (4). Since we have shown that $CD137^{pos}$ Tregs are functionally superior at regulation, an increase of this cell subset over time could result in increased peripheral regulation and increased protection from T1D. Our study has not been able to link increased accumulation with increased cell proliferation, cell survival or cell death. Although further studies are needed to understand the link between CD137 and accumulation of Tregs, our results strongly suggest that CD137 co-stimulation is important for Treg mediated diabetes prevention.

Mouse CD4^{pos}CD25^{pos} Tregs have been differentiated into subsets based on their expression of cell surface molecules such as CD134 (51), integrin alpha E beta 7(52) and CD62L (23, 53) that affect their suppressor activity, or by molecules such as CD45RA^{pos} (54) and P-selectin (55) that delineate Treg differentiation *in-vitro* or *in-vivo*. Our results differentiate two sub-populations of CD4^{pos}CD25^{pos} Tregs, CD137^{pos} and CD137^{neg}. These subsets are not merely phenotypically differentiated by cell surface expression of CD137, but by differences in functional cell mediated suppression, and by differences in the production of immunosuppressive soluble CD137.

Soluble CD137 has been reported in the sera of RA patients and in the CSF of MS patients, and MS patients have decreased expression of CD137 on their Tregs (31, 56–58). It has been shown that soluble CD137 acts to inhibit T cell proliferation (32, 33). Although the mechanism for soluble CD137 mediated suppression is not fully understood, it has been shown to bind with CD137L *in vitro* and likely mediates its effect through CD137L (32). In addition, soluble CD137 has been reported to arise later in the immune response to counteract overactivation of the immune system (33). These previous reports combined with the findings presented here suggest that production of soluble CD137 may act as a “brake” upon normal immune activation. In this scenario, activation of antigen specific CD137^{pos} Tregs could produce soluble CD137 which, in combination with contact dependent suppression, would down regulate the immune activation of both T cells and APCs expressing CD137L (59). Insufficient production of soluble CD137 (for example, in our system, mediated by a decrease in frequency of NOD Tregs producing soluble CD137 with age) could lead to exaggerated immune activation; conversely increased numbers of such Tregs could act to decrease immune activation in NOD.B10 *Idd9.3* mice. These considerations are strengthened by our observation of increased serum soluble CD137 in the protected NOD.B10 *Idd9.3* mice with age (Fig 9f), correlating with the increased accumulation of CD137^{pos} Tregs in these mice, compared to NOD mice. We showed that there was no intrinsic cellular difference between NOD and NOD.B10 *Idd9.3* cells in either contact mediated suppression (Fig 7a–c) or production of soluble CD137 (Fig 9c,d). However, the accumulation of CD137^{pos} Tregs in the NOD.B10 *Idd9.3* mice was correlated with increased total amount of serum soluble CD137 (Fig 9f) and thus increased overall immunosuppression. Similarly, while NOD and NOD.B10 *Idd9.3* CD137^{pos} Tregs do not differ in contact dependent suppression on a per cell basis (Fig 7), increased numbers of CD137^{pos} Tregs increases the total available contact mediated immunosuppression in NOD.B10 *Idd9.3* mice. Thus, the B10 *Idd9.3* allele acts primarily to enhance accumulation of CD137^{pos} cells, rather than by changing the immunosuppressive function on a per cell basis-- but the net overall effect is increased systemic immunosuppression. These conclusions are strongly supported by the evidence presented here but not directly proven, as will be done in future studies.

Our study explains how the hyporesponsive NOD CD137 allotype can contribute to increased T1D susceptibility in NOD mice, compared to the B10 allotype in the NOD.B10 *Idd9.3* mice. Thus, the NOD.B10 *Idd9.3* allele could lead to increased accumulation of functionally superior CD137^{pos} Tregs with age and thus downregulate autoimmunity; whereas NOD would have a quantitative deficiency of CD137^{pos} Tregs compared to NOD.B10 *Idd9.3,* contributing to enhanced NOD autoimmunity with age. A decreased number of CD137^{pos} Tregs results in decreased total cell mediated suppression as well as decreased production of counter-regulatory soluble CD137 (Fig 9f), which might be even more important at the site of inflammation (e.g. the pancreatic islet). These considerations lead us to suggest that enhancing site specific expression of soluble CD137 could downregulate autoimmunity, and we will explore this hypothesis in future studies.

Supplementary Material

Refer to Web version on PubMed Central for supplementary material.

Acknowledgments

We are very grateful to Oliver Burren, and Mikkel Christensen, for BAC sequencing and annotation/display. NOD.Foxp3-GFP knock-in mice were a kind gift from Vijay Kuchroo and Ana Anderson of Harvard University.

References

1. Bluestone JA, Herold K, Eisenbarth G. Genetics, pathogenesis and clinical interventions in type 1 diabetes. Nature. 2010; 464:1293–1300. [PubMed: 20432533]
2. Cannons JL, Chamberlain G, Howson J, Smink LJ, Todd JA, Peterson LB, Wicker LS, Watts TH. Genetic and functional association of the immune signaling molecule 4-1BB (CD137/TNFRSF9) with type 1 diabetes. J Autoimmun. 2005
3. Lyons PA, Hancock WW, Denny P, Lord CJ, Hill NJ, Armitage N, Siegmund T, Todd JA, Phillips MS, Hess JF, Chen SL, Fischer PA, Peterson LB, Wicker LS. The NOD Idd9 genetic interval influences the pathogenicity of insulitis and contains molecular variants of Cd30, Tnfr2, and Cd137. Immunity. 2000; 13:107–115. [PubMed: 10933399]
4. Watts TH. TNF/TNFR family members in costimulation of T cell responses. Annu Rev Immunol. 2005; 23:23–68. [PubMed: 15771565]
5. Irie J, Wu Y, Kachapati K, Mittler RS, Ridgway WM. Modulating protective and pathogenic CD4+ subsets via CD137 in type 1 diabetes. Diabetes. 2007; 56:186–196. [PubMed: 17192481]
6. Zheng G, Wang B, Chen A. The 4-1BB costimulation augments the proliferation of CD4+CD25+ regulatory T cells. J Immunol. 2004; 173:2428–2434. [PubMed: 15294956]
7. Gavin MA, Clarke SR, Negrou E, Gallegos A, Rudensky A. Homeostasis and anergy of CD4(+)CD25(+) suppressor T cells in vivo. Nat Immunol. 2002; 3:33–41. [PubMed: 11740498]
8. McHugh RS, Whitters MJ, Piccirillo CA, Young DA, Shevach EM, Collins M, Byrne MC. CD4(+)CD25(+) immunoregulatory T cells: gene expression analysis reveals a functional role for the glucocorticoid-induced TNF receptor. Immunity. 2002; 16:311–323. [PubMed: 11869690]
9. Choi BK, Bae JS, Choi EM, Kang WJ, Sakaguchi S, Vinay DS, Kwon BS. 4-1BB-dependent inhibition of immunosuppression by activated CD4+CD25+ T cells. J Leukoc Biol. 2004; 75:785–791. [PubMed: 14694186]
10. Marson A, Kretschmer K, Frampton GM, Jacobsen ES, Polansky JK, MacIsaac KD, Levine SS, Fraenkel E, von Boehmer H, Young RA. Foxp3 occupancy and regulation of key target genes during T-cell stimulation. Nature. 2007; 445:931–935. [PubMed: 17237765]
11. Chen Z, Herman AE, Matos M, Mathis D, Benoist C. Where CD4+CD25+ T reg cells impinge on autoimmune diabetes. J Exp Med. 2005; 202:1387–1397. [PubMed: 16301745]
12. Hamilton-Williams EE, Wong SB, Martinez X, Rainbow DB, Hunter KM, Wicker LS, Sherman LA. Idd9.2 and Idd9.3 protective alleles function in CD4+ T-cells and nonlymphoid cells to prevent expansion of pathogenic islet-specific CD8+ T-cells. Diabetes. 2010; 59:1478–1486. [PubMed: 20299469]
13. Elpek KG, Yolcu ES, Franke DD, Lacelle C, Schabowsky RH, Shirwan H. Ex vivo expansion of CD4+CD25+FoxP3+ T regulatory cells based on synergy between IL-2 and 4-1BB signaling. J Immunol. 2007; 179:7295–7304. [PubMed: 18025172]
14. Asseman C, Mauze S, Leach MW, Coffman RL, Powrie F. An essential role for interleukin 10 in the function of regulatory T cells that inhibit intestinal inflammation. J Exp Med. 1999; 190:995–1004. [PubMed: 10510089]
15. Mamura M, Lee W, Sullivan TJ, Felici A, Sowers AL, Allison JP, Letterio JJ. CD28 disruption exacerbates inflammation in Tgf-beta1−/−mice: in vivo suppression by CD4+CD25+ regulatory T cells independent of autocrine TGF-beta1. Blood. 2004; 103:4594–4601. [PubMed: 15016653]

16. Garin MI, Chu CC, Golshayan D, Cernuda-Morollon E, Wait R, Lechler RI. Galectin-1: a key effector of regulation mediated by CD4+CD25+ T cells. Blood. 2007; 109:2058–2065. [PubMed: 17110462]
17. Collison LW, Workman CJ, Kuo TT, Boyd K, Wang Y, Vignali KM, Cross R, Sehy D, Blumberg RS, Vignali DA. The inhibitory cytokine IL-35 contributes to regulatory T-cell function. Nature. 2007; 450:566–569. [PubMed: 18033300]
18. Baratelli F, Lin Y, Zhu L, Yang SC, Heuze-Vourc'h N, Zeng G, Reckamp K, Dohadwala M, Sharma S, Dubinett SM. Prostaglandin E2 induces FOXP3 gene expression and T regulatory cell function in human CD4+ T cells. J Immunol. 2005; 175:1483–1490. [PubMed: 16034085]
19. Chaturvedi V, Collison LW, Guy CS, Workman CJ, Vignali DA. Cutting edge: Human regulatory T cells require IL-35 to mediate suppression and infectious tolerance. J Immunol. 2011; 186:6661–6666. [PubMed: 21576509]
20. Chauhan SK, Saban DR, Lee HK, Dana R. Levels of Foxp3 in regulatory T cells reflect their functional status in transplantation. J Immunol. 2009; 182:148–153. [PubMed: 19109145]
21. Chen ML, Yan BS, Bando Y, Kuchroo VK, Weiner HL. Latency-associated peptide identifies a novel CD4+CD25+ regulatory T cell subset with TGFbeta-mediated function and enhanced suppression of experimental autoimmune encephalomyelitis. J Immunol. 2008; 180:7327–7337. [PubMed: 18490732]
22. Collison LW, Pillai MR, Chaturvedi V, Vignali DA. Regulatory T cell suppression is potentiated by target T cells in a cell contact, IL-35-and IL-10-dependent manner. J Immunol. 2009; 182:6121–6128. [PubMed: 19414764]
23. Fu S, Yopp AC, Mao X, Chen D, Zhang N, Mao M, Ding Y, Bromberg JS. CD4+ CD25+ CD62+ T-regulatory cell subset has optimal suppressive and proliferative potential. Am J Transplant. 2004; 4:65–78. [PubMed: 14678036]
24. Jonuleit H, Schmitt E, Kakirman H, Stassen M, Knop J, Enk AH. Infectious tolerance: human CD25(+) regulatory T cells convey suppressor activity to conventional CD4(+) T helper cells. J Exp Med. 2002; 196:255–260. [PubMed: 12119350]
25. Kim YG, Lee CK, Nah SS, Mun SH, Yoo B, Moon HB. Human CD4+CD25+ regulatory T cells inhibit the differentiation of osteoclasts from peripheral blood mononuclear cells. Biochem Biophys Res Commun. 2007; 357:1046–1052. [PubMed: 17462597]
26. Lin J, Li M, Wang Z, He S, Ma X, Li D. The role of CD4+CD25+ regulatory T cells in macrophage-derived foam-cell formation. J Lipid Res. 2010; 51:1208–1217. [PubMed: 20007839]
27. Strauss L, Bergmann C, Szczepanski MJ, Lang S, Kirkwood JM, Whiteside TL. Expression of ICOS on human melanoma-infiltrating CD4+CD25highFoxp3+ T regulatory cells: implications and impact on tumor-mediated immune suppression. J Immunol. 2008; 180:2967–2980. [PubMed: 18292519]
28. Sun L, Yi S, O'Connell PJ. Foxp3 regulates human natural CD4+CD25+ regulatory T-cell-mediated suppression of xenogeneic response. Xenotransplantation. 2010; 17:121–130. [PubMed: 20522244]
29. Szczepanski MJ, Szajnik M, Czystowska M, Mandapathil M, Strauss L, Welsh A, Foon KA, Whiteside TL, Boyiadzis M. Increased frequency and suppression by regulatory T cells in patients with acute myelogenous leukemia. Clin Cancer Res. 2009; 15:3325–3332. [PubMed: 19417016]
30. Setareh M, Schwarz H, Lotz M. A mRNA variant encoding a soluble form of 4-1BB, a member of the murine NGF/TNF receptor family. Gene. 1995; 164:311–315. [PubMed: 7590349]
31. Jung HW, Choi SW, Choi JI, Kwon BS. Serum concentrations of soluble 4-1BB and 4-1BB ligand correlated with the disease severity in rheumatoid arthritis. Exp Mol Med. 2004; 36:13–22. [PubMed: 15031666]
32. Shao Z, Sun F, Koh DR, Schwarz H. Characterisation of soluble murine CD137 and its association with systemic lupus. Mol Immunol. 2008; 45:3990–3999. [PubMed: 18640726]
33. Michel J, Schwarz H. Expression of soluble CD137 correlates with activation-induced cell death of lymphocytes. Cytokine. 2000; 12:742–746. [PubMed: 10843756]
34. Hamilton-Williams EE, Martinez X, Clark J, Howlett S, Hunter KM, Rainbow DB, Wen L, Shlomchik MJ, Katz JD, Beilhack GF, Wicker LS, Sherman LA. Expression of diabetes-

associated genes by dendritic cells and CD4 T cells drives the loss of tolerance in nonobese diabetic mice. J Immunol. 2009; 183:1533–1541. [PubMed: 19592648]

35. Bettelli E, Carrier Y, Gao W, Korn T, Strom TB, Oukka M, Weiner HL, Kuchroo VK. Reciprocal developmental pathways for the generation of pathogenic effector TH17 and regulatory T cells. Nature. 2006; 441:235–238. [PubMed: 16648838]
36. Foell J, McCausland M, Burch J, Corriazzi N, Yan XJ, Suwyn C, O'Neil SP, Hoffmann MK, Mittler RS. CD137-mediated T cell co-stimulation terminates existing autoimmune disease in SLE-prone NZB/NZW F1 mice. Ann N Y Acad Sci. 2003; 987:230–235. [PubMed: 12727643]
37. Steward CA, Humphray S, Plumb B, Jones MC, Quail MA, Rice S, Cox T, Davies R, Bonfield J, Keane TM, Nefedov M, de Jong PJ, Lyons P, Wicker L, Todd J, Hayashizaki Y, Gulban O, Danska J, Harrow J, Hubbard T, Rogers J, Adams DJ. Genome-wide end-sequenced BAC resources for the NOD/MrkTac() and NOD/ShiLtJ() mouse genomes. Genomics. 2010; 95:105–110. [PubMed: 19909804]
38. Ning Z, Cox AJ, Mullikin JC. SSAHA: a fast search method for large DNA databases. Genome Res. 2001; 11:1725–1729. [PubMed: 11591649]
39. Hulbert EM, Smink LJ, Adlem EC, Allen JE, Burdick DB, Burren OS, Cassen VM, Cavnor CC, Dolman GE, Flamez D, Friery KF, Healy BC, Killcoyne SA, Kutlu B, Schuilenburg H, Walker NM, Mychaleckyj J, Eizirik DL, Wicker LS, Todd JA, Goodman N. T1DBase: integration and presentation of complex data for type 1 diabetes research. Nucleic Acids Res. 2007; 35:D742–746. [PubMed: 17169983]
40. Smink LJ, Helton EM, Healy BC, Cavnor CC, Lam AC, Flamez D, Burren OS, Wang Y, Dolman GE, Burdick DB, Everett VH, Glusman G, Laneri D, Rowen L, Schuilenburg H, Walker NM, Mychaleckyj J, Wicker LS, Eizirik DL, Todd JA, Goodman N. T1DBase, a community web-based resource for type 1 diabetes research. Nucleic Acids Res. 2005; 33:D544–549. [PubMed: 15608258]
41. Stein LD, Mungall C, Shu S, Caudy M, Mangone M, Day A, Nickerson E, Stajich JE, Harris TW, Arva A, Lewis S. The generic genome browser: a building block for a model organism system database. Genome Res. 2002; 12:1599–1610. [PubMed: 12368253]
42. Lee HW, Park SJ, Choi BK, Kim HH, Nam KO, Kwon BS. 4-1BB promotes the survival of CD8+ T lymphocytes by increasing expression of Bcl-xL and Bfl-1. J Immunol. 2002; 169:4882–4888. [PubMed: 12391199]
43. Bertram EM, Lau P, Watts TH. Temporal segregation of 4-1BB versus CD28-mediated costimulation: 4-1BB ligand influences T cell numbers late in the primary response and regulates the size of the T cell memory response following influenza infection. J Immunol. 2002; 168:3777–3785. [PubMed: 11937529]
44. Pop SM, Wong CP, Culton DA, Clarke SH, Tisch R. Single cell analysis shows decreasing FoxP3 and TGFbeta1 coexpressing CD4+CD25+ regulatory T cells during autoimmune diabetes. J Exp Med. 2005; 201:1333–1346. [PubMed: 15837817]
45. Kim J, Choi SP, La S, Seo JS, Kim KK, Nam SH, Kwon B. Constitutive expression of 4-1BB on T cells enhances CD4+ T cell responses. Exp Mol Med. 2003; 35:509–517. [PubMed: 14749528]
46. Mellanby RJ, Thomas D, Phillips JM, Cooke A. Diabetes in non-obese diabetic mice is not associated with quantitative changes in CD4+ CD25+ Foxp3+ regulatory T cells. Immunology. 2007; 121:15–28. [PubMed: 17428252]
47. Cannons JL, Lau P, Ghumman B, DeBenedette MA, Yagita H, Okumura K, Watts TH. 4-1BB ligand induces cell division, sustains survival, and enhances effector function of CD4 and CD8 T cells with similar efficacy. J Immunol. 2001; 167:1313–1324. [PubMed: 11466348]
48. Hurtado JC, Kim YJ, Kwon BS. Signals through 4-1BB are costimulatory to previously activated splenic T cells and inhibit activation-induced cell death. J Immunol. 1997; 158:2600–2609. [PubMed: 9058792]
49. Gregg RK, Jain R, Schoenleber SJ, Divekar R, Bell JJ, Lee HH, Yu P, Zaghouani H. A sudden decline in active membrane-bound TGF-beta impairs both T regulatory cell function and protection against autoimmune diabetes. J Immunol. 2004; 173:7308–7316. [PubMed: 15585854]

50. Thomas DC, Mellanby RJ, Phillips JM, Cooke A. An early age-related increase in the frequency of CD4+ Foxp3+ cells in BDC2.5NOD mice. Immunology. 2007; 121:565–576. [PubMed: 17437531]

51. Nolte-'t, Hoen EN.; Wagenaar-Hilbers, JP.; Boot, EP.; Lin, CH.; Arkesteijn, GJ.; van Eden, W.; Taams, LS.; Wauben, MH. Identification of a CD4+CD25+ T cell subset committed in vivo to suppress antigen-specific T cell responses without additional stimulation. Eur J Immunol. 2004; 34:3016–3027. [PubMed: 15376196]

52. Lehmann J, Huehn J, de la Rosa M, Maszyna F, Kretschmer U, Krenn V, Brunner M, Scheffold A, Hamann A. Expression of the integrin alpha Ebeta 7 identifies unique subsets of CD25+ as well as CD25-regulatory T cells. Proc Natl Acad Sci U S A. 2002; 99:13031–13036. [PubMed: 12242333]

53. Szanya V, Ermann J, Taylor C, Holness C, Fathman CG. The subpopulation of CD4+CD25+ splenocytes that delays adoptive transfer of diabetes expresses L-selectin and high levels of CCR7. J Immunol. 2002; 169:2461–2465. [PubMed: 12193715]

54. Hoffmann P, Eder R, Boeld TJ, Doser K, Piseshka B, Andreesen R, Edinger M. Only the CD45RA + subpopulation of CD4+CD25high T cells gives rise to homogeneous regulatory T-cell lines upon in vitro expansion. Blood. 2006; 108:4260–4267. [PubMed: 16917003]

55. Kohm AP, Miller SD. Role of ICAM-1 and P-selectin expression in the development and effector function of CD4+CD25+regulatory T cells. J Autoimmun. 2003; 21:261–271. [PubMed: 14599851]

56. Liu GZ, Gomes AC, Fang LB, Gao XG, Hjelmstrom P. Decreased 4-1BB expression on CD4+CD25 high regulatory T cells in peripheral blood of patients with multiple sclerosis. Clin Exp Immunol. 2008; 154:22–29. [PubMed: 18727631]

57. Liu GZ, Gomes AC, Putheti P, Karrenbauer V, Kostulas K, Press R, Hillert J, Hjelmstrom P, Gao XG. Increased soluble 4-1BB ligand (4-1BBL) levels in peripheral blood of patients with multiple sclerosis. Scand J Immunol. 2006; 64:412–419. [PubMed: 16970683]

58. Sharief MK. Heightened intrathecal release of soluble CD137 in patients with multiple sclerosis. Eur J Neurol. 2002; 9:49–54. [PubMed: 11784376]

59. Hurtado JC, Kim SH, Pollok KE, Lee ZH, Kwon BS. Potential role of 4-1BB in T cell activation. Comparison with the costimulatory molecule CD28. J Immunol. 1995; 155:3360–3367. [PubMed: 7561030]

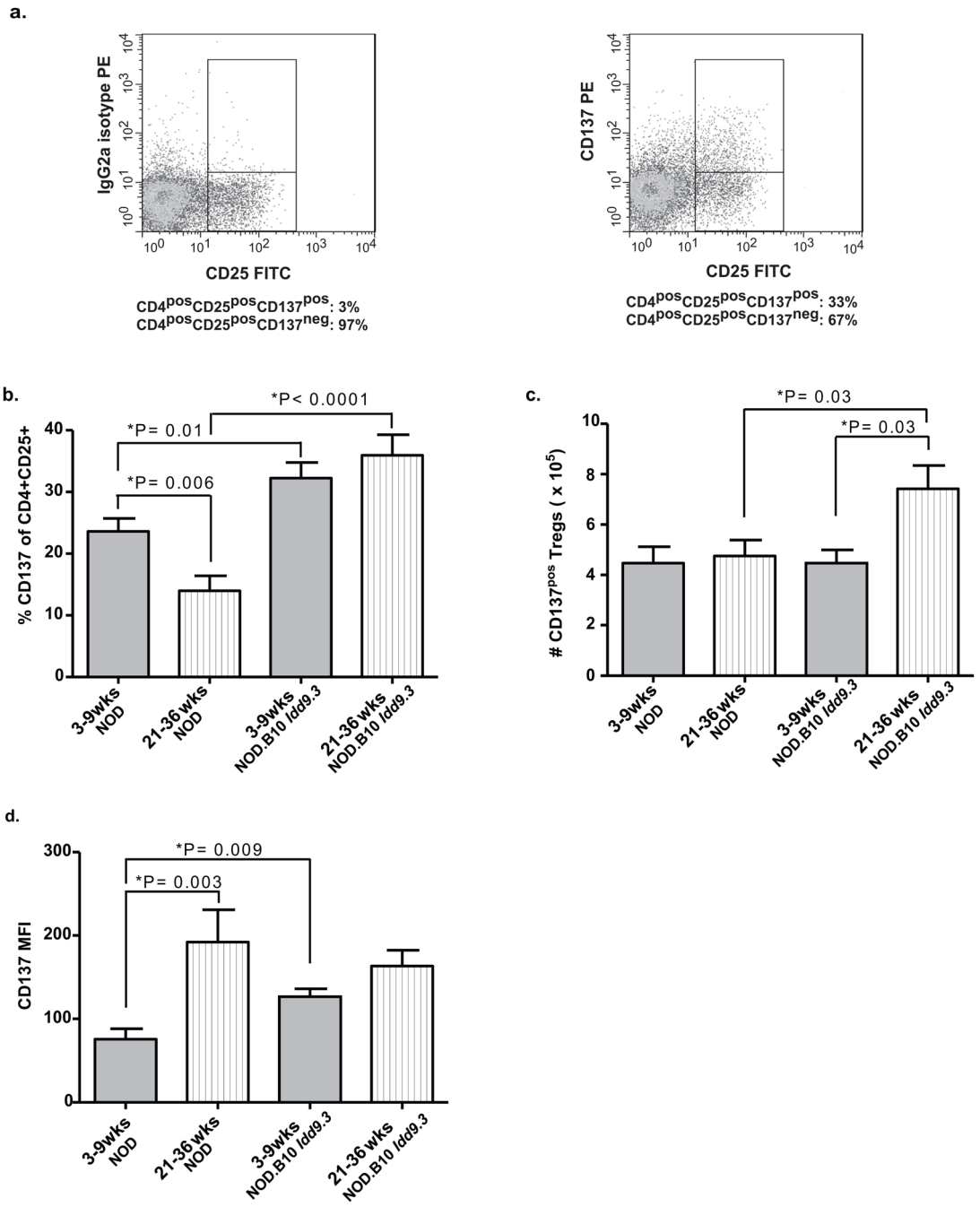

Figure one. Percentages and absolute numbers of CD137^{pos}CD4^{pos}CD25^{pos} T cells are significantly lower in aged NOD versus NOD.B10 *Idd9.3* mice

(a) Splenocytes from six week old NOD mice were stained with CD4-APC, CD25-FITC and anti-CD137-PE or IgG2a isotype control, and analyzed by flow cytometry. The IgG2a istoype control staining was used to establish true CD137 staining. Percentages below the figure show the percent CD137^{pos} vs. CD137^{neg} in the CD4^{pos}CD25^{pos} gate. One representative of multiple experiments. (b, c, d) NOD and NOD.B10 *Idd9.3* splenocytes were isolated from younger (3–9 week) and older (21–36 week) non-diabetic females, stained with CD4-APC, CD25-FITC and anti-CD137-PE and analyzed by flow cytometry. (b) Isotype staining was used to gate for percentage of CD137^{pos} T cells in the

CD4^{pos}CD25^{pos}T cell subset in NOD (n=18, 3–9 wk old and n=12, 21–36 wk old mice) and NOD.B10 *Idd9.3* (n=12, 3–9 wk old and n=16, 21–36 wk old) spleen. (c) The number of CD4^{pos}CD25^{pos}CD137^{pos} T cells was counted in NOD (n=8, 3–9 wk old and n=7, 21–36 wk old) and NOD.B10 *Idd9.3* (n=5, 3–9 wk old and n=7, 21–36 wk old) spleen. (d) The mean florescence intensity of CD137 on CD137^{pos}CD4^{pos}CD25^{pos} T cells was analyzed on NOD (n=10, 3–9 wk old and n=5, 21–36 wk) and NOD.B10 *Idd9.3* (n=7, 3–9 wk old and n=9, 21–36 wk old mice) spleen.

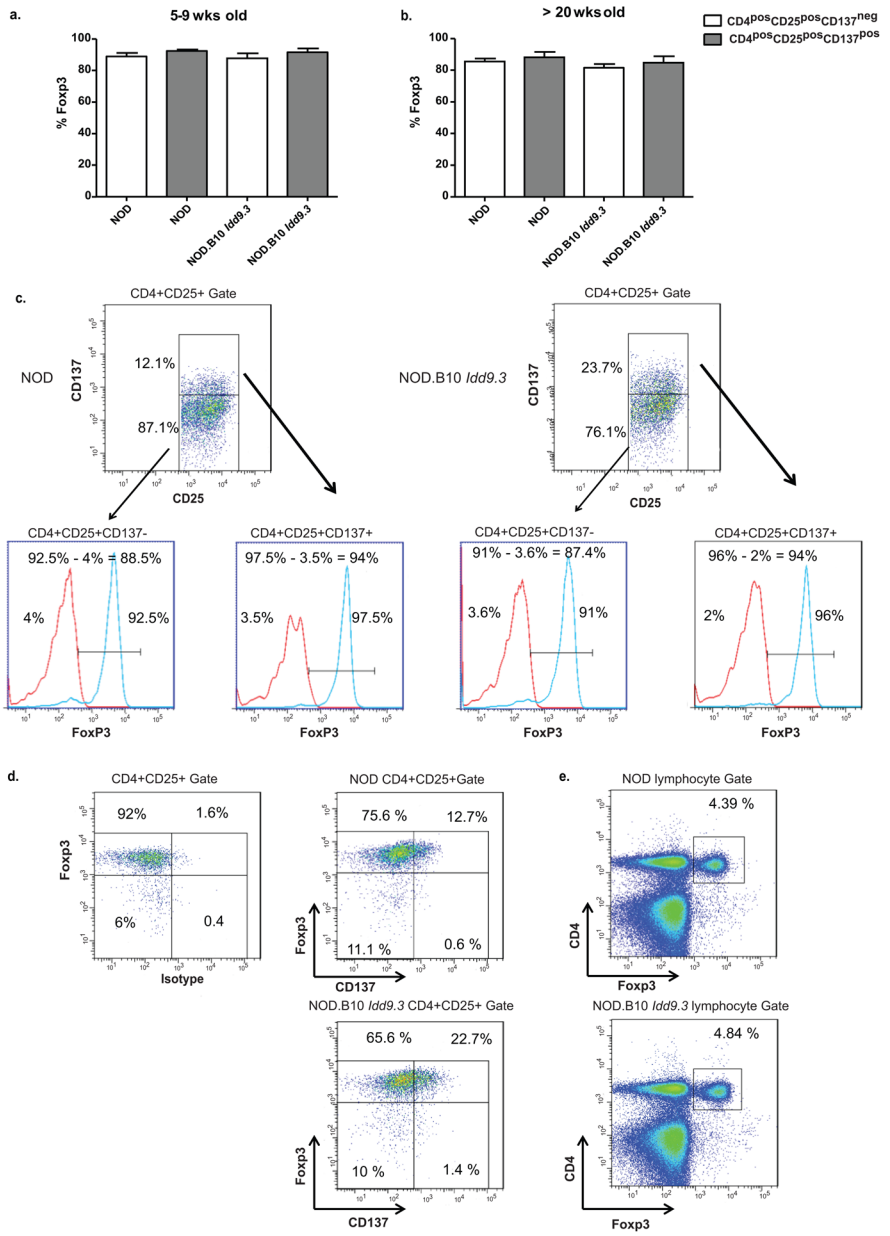

Figure two. NOD and NOD.B10 *Idd9.3* CD4^{pos}CD25^{pos} Treg subsets show no difference in intracellular Foxp3 staining

(a, b) Splenocytes from 5–9 week old NOD (n=3) and NOD.B10 *Idd9.3* (n=2) and 20–30 wk old NOD (n=4) and NOD.B10 *Idd9.3* (n=6) female mice were surface stained with CD4-APC.Cy7, CD25-Percep-Cy5.5 and anti-CD137APC, followed by intracellular staining for Foxp3-PE or IgG2a isotype control. (The CD137 gates are based on isotype staining for CD137, as shown in Fig 1a). (c) Representative dot plots of the FACS gating used to calculate the percent Foxp3 staining in parts (a) and (b) using seven week old NOD (left) and six week old NOD.B10 *Idd9.3* (right). Within the CD4^{pos}CD25^{pos} gate, the CD4^{pos}CD25^{pos}CD137^{neg} and CD4^{pos}CD25^{pos}CD137^{pos} Tregs were gated for Foxp3 or isotype histograms. The isotype histogram was used to establish gates for Foxp3 positive staining. The percent overlapping isotype staining in the gate was subtracted from the percent Foxp3+ in the gate (as noted on the top of each histogram) to calculate the true

percent Foxp3 shown in Figure 2a, b. (d) The same NOD and NOD.B10 *Idd9.3* mice used in Figure 2c were gated for $CD4^{pos}CD25^{pos}$ T cells to show representative dot plots of Foxp3 and isotype (left) or Foxp3 and CD137 (middle). e) Representative dot plots of CD4 and Foxp3 within the lymphocyte gate of the same NOD and NOD.B10 *Idd9.3* mice used in Figure 2c.

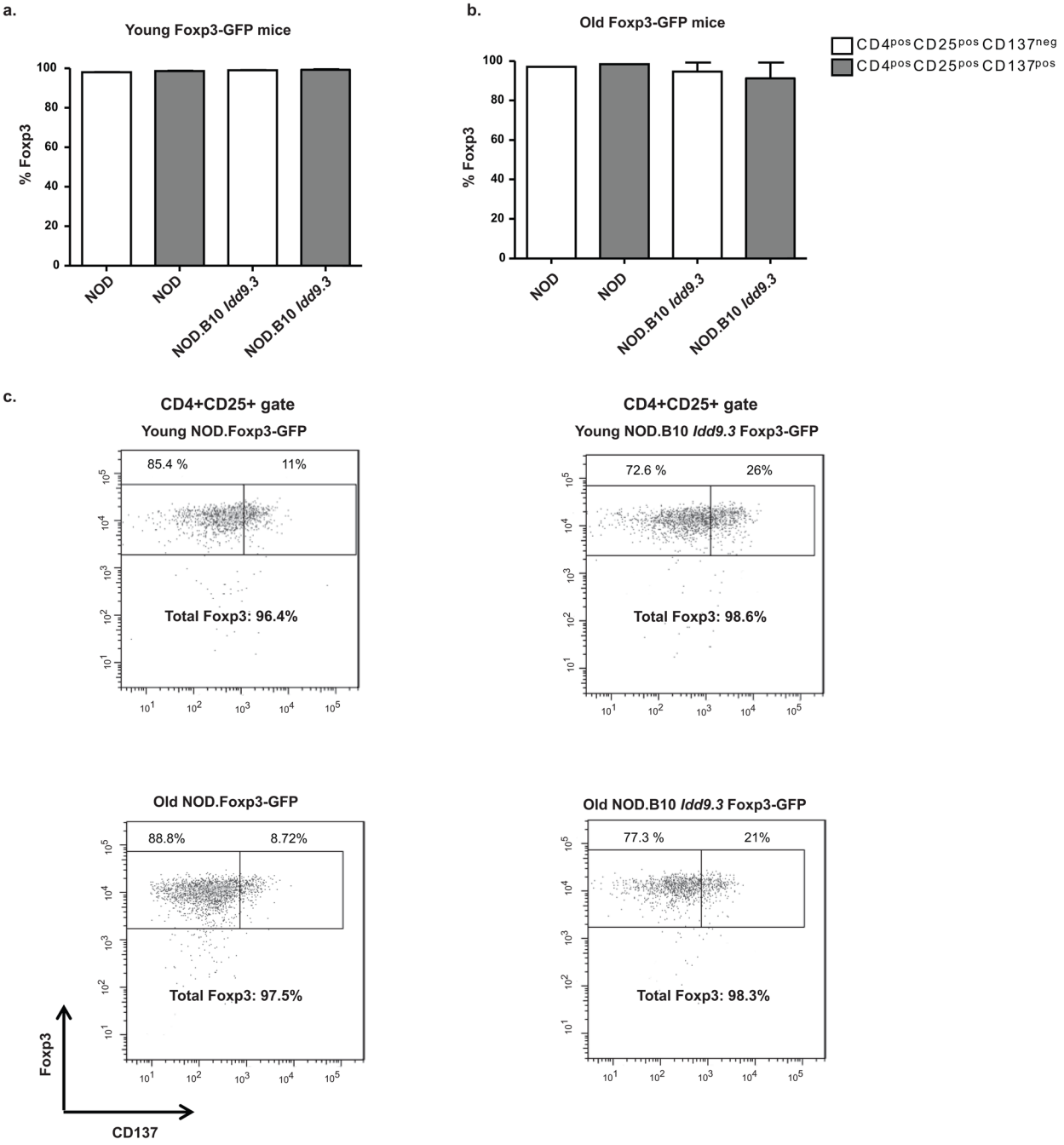

Figure three. NOD.Foxp3-GFP and NOD.B10 *Idd9.3* Foxp3-GFP mice demonstrate that the majority of $CD4^{pos}CD25^{pos}CD137^{pos}$ cells are Foxp3 Tregs and that there is no significant difference in the percent Foxp3+ cells between NOD and NOD.B10 *Idd9.3.*

(a, b) Splenocytes from NOD.Foxp3-GFP (n=3, 3–9 wk old and n=2, 21–25 wk old) and NOD.B10 *Idd9.3*.Foxp3-GFP (n=3, 3–9 wk old and n=3, 21–25 wk old) were stained for CD4-APC-Cy7, CD25-Percep-Cy5.5 and CD137-APC or IgG2a isotype control. The cells were analyzed for Foxp3-GFP expression in $CD137^{pos}$ and $CD137^{neg}$ Tregs in (a) 3–9 week and (b) 21–25 week old mice. (c) Representative dot plots showing Foxp3/CD137 staining within CD4+CD25+ gate for each strain and age group shown in section a and b. FACS staining and gating were used to calculate the percent Foxp3 in the $CD137^{neg}$ and $CD137^{pos}$

subsets from young (top) and old (bottom) NOD.Foxp3-GFP (left) and NOD.B10 *Idd9.3*.Foxp3-GFP (right). (The CD137 gates are based on isotype staining for CD137, as shown in Fig 1a).

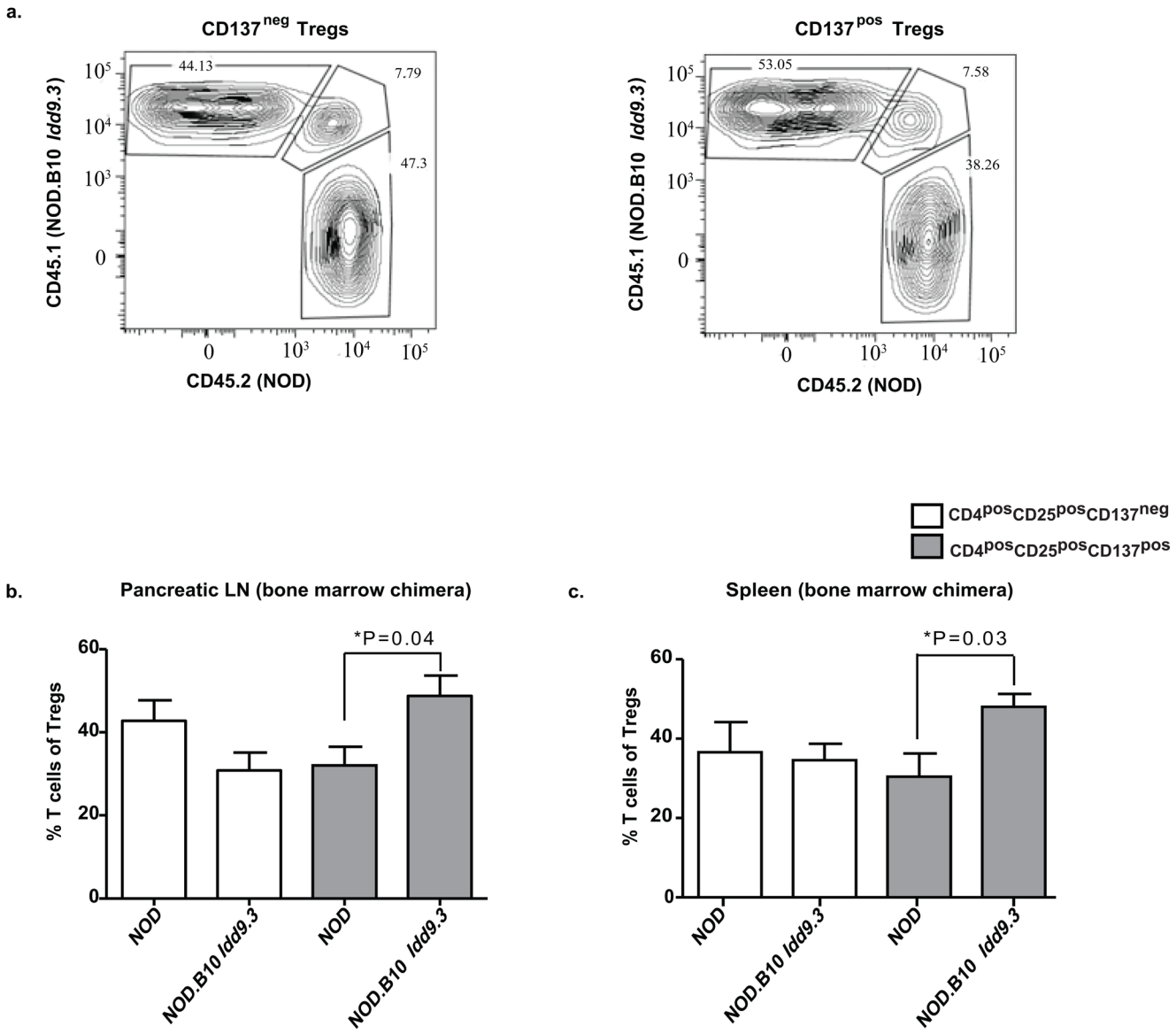

Figure four. CD137^{pos} Tregs expressing the B10 *Idd9.3* region demonstrate an intrinsic cell accumulation in mixed bone marrow chimeric mice

15–25 million bone marrow cells from 5–12 week old NOD.B10 *Idd9.3* mice and NOD.CD45.2 mice were mixed at 1:1 ratio and injected into 9–13 week old irradiated (800–1200 Rads in different experiments) (NOD.CD45.2 X NOD.B10 *Idd9.3*) F1 mice. Recipient non-diabetic mice were sacrificed 12–20 weeks after reconstitution. (a) One representative experiment showing the expression of the CD45.1 (NOD.B10 *Idd9.3*) vs. CD45.2 (NOD) allotype by CD137^{neg} (left) and CD137^{pos} (right) Tregs 12 weeks after reconstitution of the bone marrow chimera. (b) Spleen (n=5), and (c) pancreatic lymph nodes (n=4) were harvested and stained with CD4-APC-Cy7, CD25-Percp-Cy5.5, CD45.1-APC, CD45.2-FITC and anti-CD137-PE and analyzed on a FACS Cantos cytometer. Percentage of each F1 (host) cells not shown. Statistical significance was calculated using the unpaired t test.

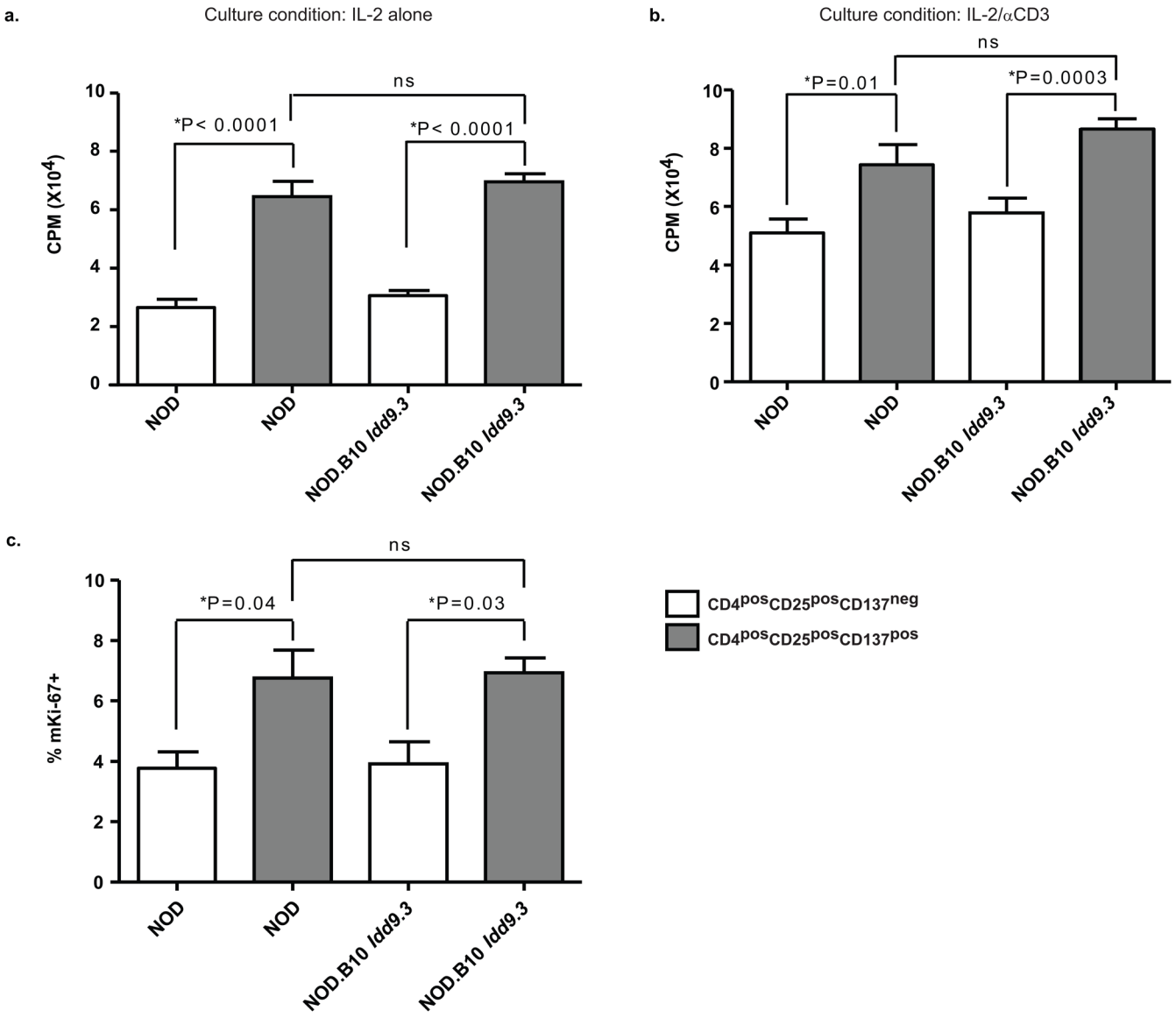

Figure five. No proliferative differences between NOD and NOD.B10 *Idd9.3* CD137^{pos} Tregs *ex vivo* or *in vitro*

(a, b) Splenocytes from 4–6 week old NOD and NOD.B10 *Idd9.3* females were stained with CD4-APC-Cy7, CD25-Percep-Cy5.5, and anti-CD137-APC, and FACS-sorted for CD4^{pos}CD25^{pos}CD137^{neg} and CD4^{pos}CD25^{pos}CD137^{pos} cells. 50,000 sorted cells were cultured with (a) 25U/ml IL-2 or (b) 25U/ml IL-2 and 1.25 ug/ml anti-CD3 in triplicate wells. The cells were pulsed with ^{3}H labeled thymidine on day 3 and harvested after 16 hours and the data was pooled from n=3 experiments. (c) Splenocytes from 5–7 week old NOD (n=3) and NOD.B10 *Idd9.3* (n=3) females were surface stained with CD4-APC-Cy7, CD25-Percep-Cy5.5 and anti-CD137-APC, followed by intracellular staining for Ki-67-Alexa-488. The stained cells were analyzed by flow cytometry. Statistical significance was calculated with the unpaired t test.

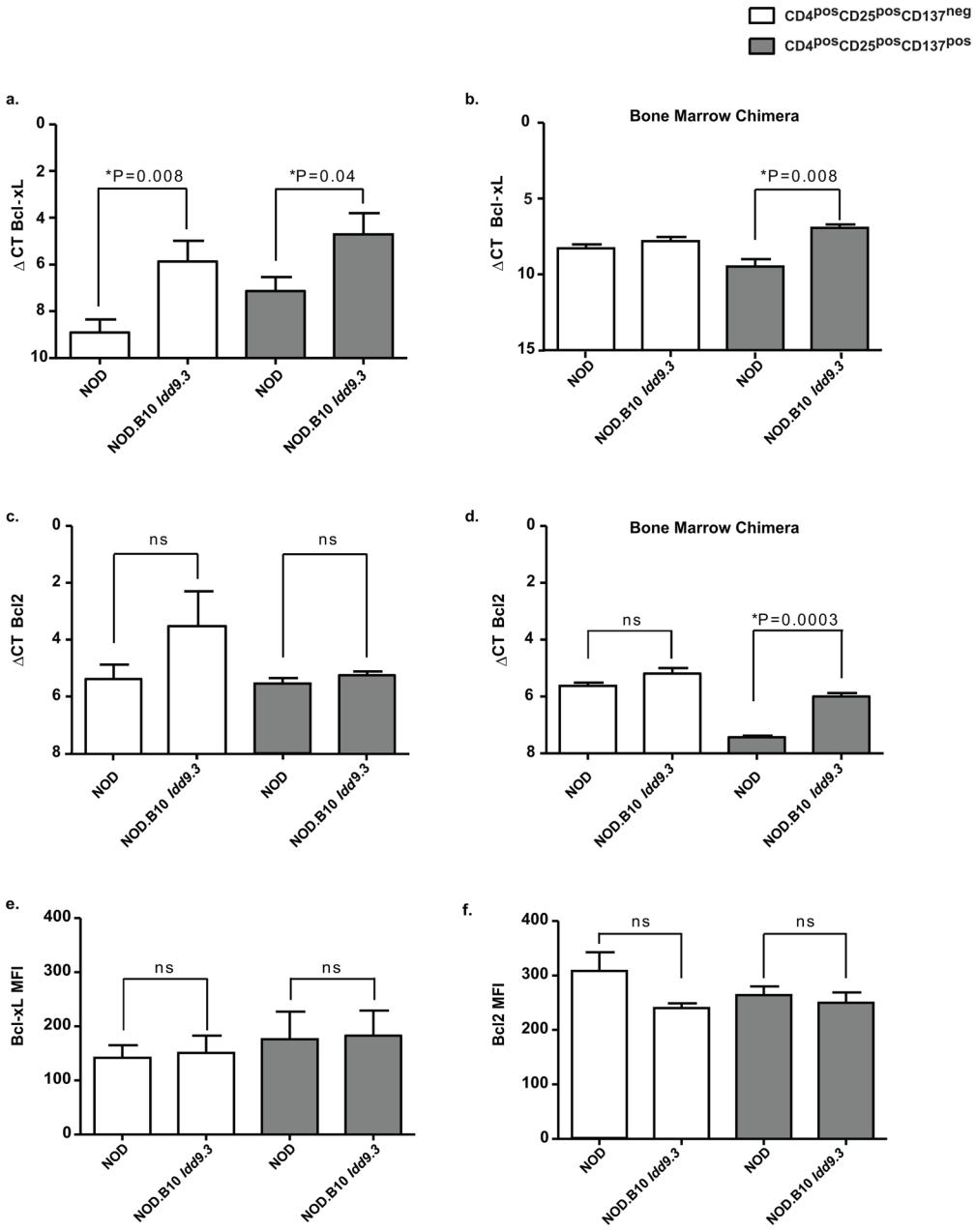

Figure six. Peripheral NOD.B10 *Idd9.3* CD137^{pos} Tregs express higher levels of Bcl-xL mRNA than NOD CD137^{pos} Tregs

(a) Splenocytes from 4–7 week old NOD (n=9) and NOD.B10 *Idd9.3* (n=6) females were used for sorting up-to 50,000 CD4^{pos}CD25^{neg}CD137^{neg}, CD4^{pos}CD25^{pos}CD137^{neg} and CD4^{pos}CD25^{pos}CD137^{pos} cells as described above. RNA was extracted from the sorted cells and converted to cDNA as described in the methods. Quantitative Real Time Polymerase Chain Reaction (RTPCR) was performed on the cDNA using either B2m or Gapdh and Bcl-xL primers. (b) NOD.B10 *Idd9.3* and NOD.CD45.2 mixed bone marrow chimeric mice were made as above. Recipient non-diabetic mice were sacrificed 9–10 week post injection. CD137^{neg} and CD137^{pos} Tregs were sorted according to their CD45.1 (NOD.B10 *Idd9.3*) and CD45.2 (NOD) allotype and used for RT-PCR with B2m and Bcl-xL primers. The mean of (n=3) separate experiments is shown. (c) 4–7 week old NOD (n=3) and NOD.B10 *Idd9.3*

(n=3) female splenocytes were used for sorting 50,000 $CD4^{pos}CD25^{neg}CD137^{neg}$, $CD4^{pos}CD25^{pos}CD137^{neg}$ and $CD4^{pos}CD25^{pos}CD137^{pos}$ cells and used for RT-PCR with B2m and Bcl2 primers. (d) CD45.1 or CD45.2 expressing $CD137^{neg}$ and $CD137^{pos}$ Tregs were sorted from mixed bone marrow chimera as in (b) and used for RT-PCR with B2m and Bcl2 (n=3). (e, f) Splenocytes from 4–9 week old NOD (n=4) and NOD.B10 *Idd9.3* (n=3) females were surface stained with CD4APC.Cy7, CD25Percep-Cy5.5 and anti-CD137APC, followed by intracellular staining for Bcl-xL Alexa-Fluor 488 (e) or Bcl2 Alexa-Fluor 488 (f) and their matched isotype control. The stained cells were analyzed by flow cytometry for MFI for Bcl-xL or Bcl2 within $CD4^{pos}CD25^{pos}CD137^{neg}$ and $CD4^{pos}CD25^{pos}CD137^{pos}$ cells. All statistical calculations were performed using the unpaired t test.

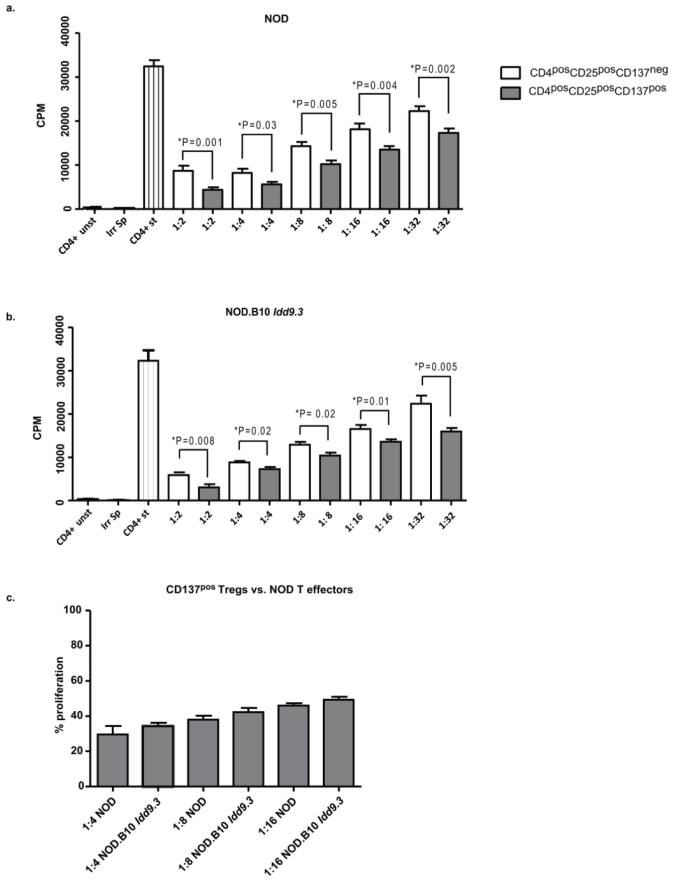

Figure seven. CD137^{pos} Tregs are functionally superior to CD137^{neg} Tregs in contact-dependent mechanism in NOD and NOD.B10 *Idd9.3 mice,* but there is no difference between NOD and NOD.B10 *Idd9.3* CD137^{pos} Treg suppressive function

(a, b) CD4^{pos}CD25^{neg}CD137^{neg} T cells and CD137^{neg} and CD137^{pos} Tregs were sorted from spleen of 4–12 week old NOD and NOD.B10 *Idd9.3* female mice as described in the methods. 50,000 CD4^{pos}CD25^{neg}CD137^{neg} T cells were plated in U-bottom 96 well plates with 1.25 ug/well soluble anti-CD3, 50,000 irradiated (1500 rads) syngeneic splenocytes and titrated numbers of syngeneic CD137^{neg} or CD137^{pos} Tregs. Unstimulated CD4^{pos}CD25^{neg}CD137^{neg} T cells and irradiated splenocytes alone were used as negative controls. The cells were pulsed with ^{3}H labeled thymidine on day 3 and harvested after 16 hours. (a) For NOD, the data was pooled from n=10 experiments for 1:2 (CD4 T cell: Treg ratio), n=7 experiments for 1:4, n=8 experiments for 1:8, n=8 experiments for 1:16 and n=7 experiments for 1:32. (b) For NOD.B10 *Idd9.3*, the data was pooled from n=3 experiments for 1:2, n=2 experiments for 1:4, n=3 experiments for 1:8, n=4 experiments for 1:16 and n=5 experiments for 1:32. (c) CD4^{pos}CD25^{neg}CD137^{neg} T cells and CD137^{pos} Tregs were sorted from spleen of 5–8 week old NOD and NOD.B10 *Idd9.3* females as described above. 50,000 NOD CD4^{pos}CD25^{neg}CD137^{neg} T cells were plated in U-bottom 96 well plates with 1.25 ug/well soluble anti-CD3, 50,000 irradiated (1500 rads) NOD splenocytes and titrated numbers of NOD or NOD.B10 *Idd9.3* CD137^{pos} Tregs. The cells were pulsed with ^{3}H labeled thymidine on day 3 and harvested after 16 hours. The percentage proliferation was calculated by dividing the CPM counts in wells with Tregs by the mean CPM count of the wells containing only CD4^{pos}CD25^{neg}CD137^{neg} T cells. The data was pooled from n=2 experiments for 1:4 and n=5 experiments for 1:8 and 1:16 for both NOD and NOD.B10 *Idd9.3* mice. Statistical significance was calculated with the unpaired t test.

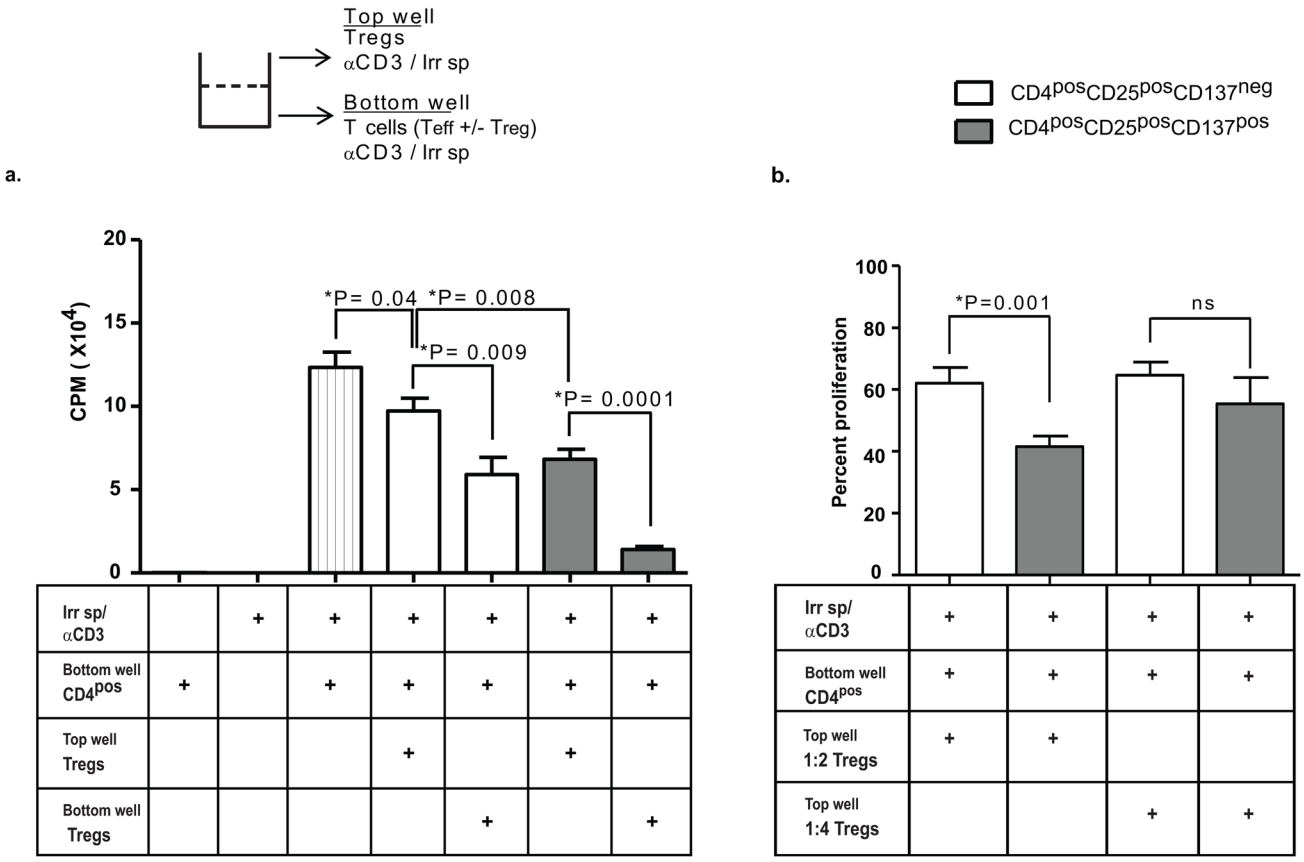

Figure eight. CD137^{pos} Tregs are functionally superior to CD137^{neg} Tregs in contact-independent suppression

(a) NOD CD4^{pos}CD25^{neg}CD137^{neg} T cells and CD137^{neg} and CD137^{pos} Tregs were sorted from 5–9 week old mice as described above. 100,000 CD4^{pos}CD25^{neg}CD137^{neg} T cells were plated in the bottom of 96 well transwell plates with 1 ug/well soluble anti-CD3, and 50,000 CD137^{neg} or CD137^{pos} Tregs were cultured in either the top wells (columns four and six, testing for soluble suppression) or the bottom wells (columns five and seven, producing a standard contact dependent suppression as in Fig 7). 100,000 irradiated (1500 Rads) splenocytes were added to both the bottom and top transwells. The cells in the bottom well were pulsed with 3H-labeled thymidine on day 3 and harvested after 16 hours (n=3 experiments for all conditions). Control wells contained either CD4^{pos} cells alone (first column), irradiated splenocytes alone (second column) or no Tregs (third column). (b) Mean percent proliferation in transwell suppression assays performed at 1:2 (n=10) and 1:4 (n=3) ratios of Treg: T cell. The percentage proliferation was calculated by dividing the CPM counts of the wells containing Tregs by the mean CPM count of the wells with only CD4^{pos}CD25^{neg}CD137^{neg} T cells. Statistical analysis performed using the unpaired T test.

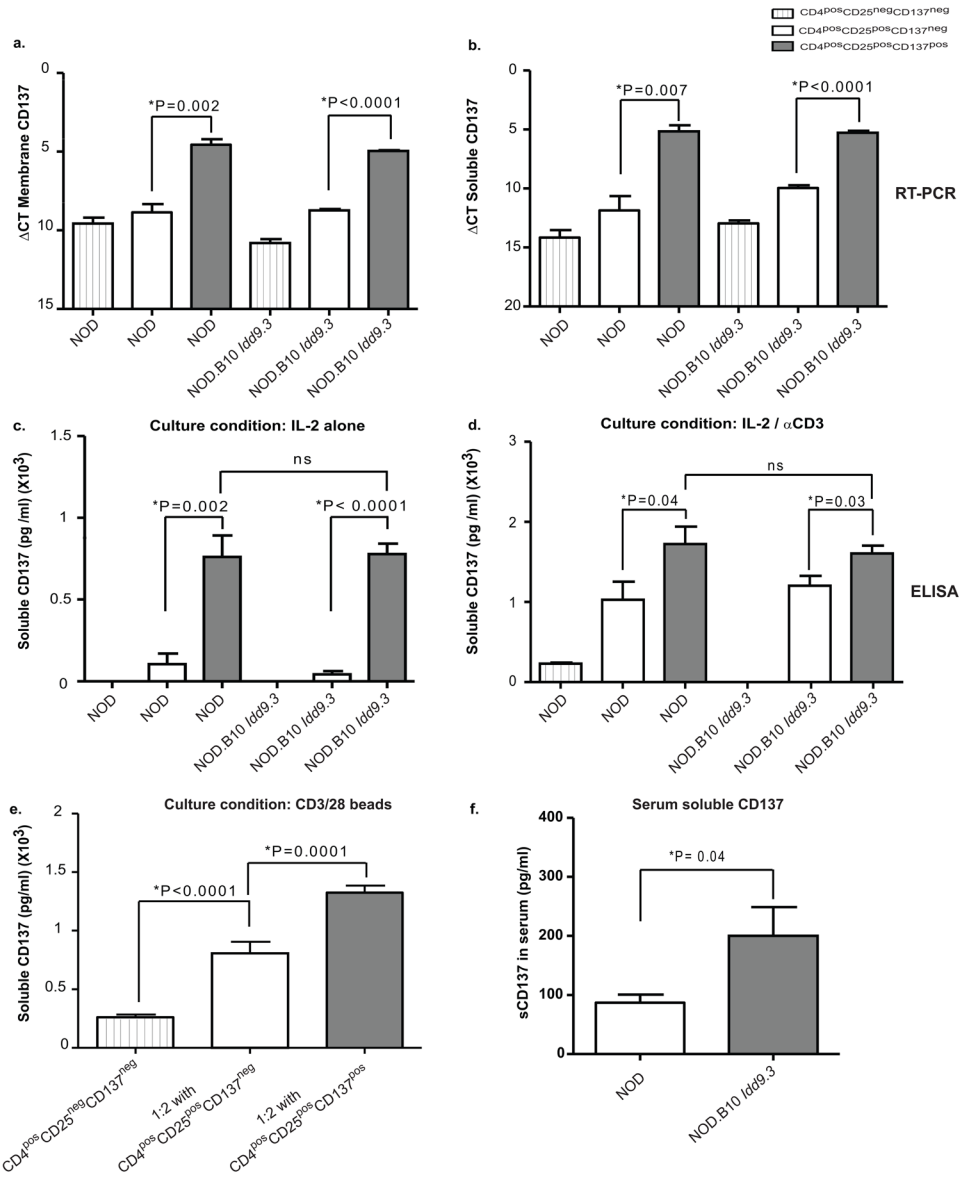

Figure nine. NOD and NOD.B10 *Idd*9.3 CD137^{pos} Tregs are the major cellular source of soluble CD137 *ex-vivo; NOD.B10* Idd9.3 *congenic mice have higher serum soluble CD137 levels than NOD.*

(a, b) RT-PCR for soluble and membrane CD137: NOD and NOD.B10 *Idd*9.3 CD4^{pos}CD25^{neg}CD137^{neg}, CD4^{pos}CD25^{pos}CD137^{neg} and CD4^{pos}CD25^{pos}CD137^{pos} T cells were sorted from 4–8 week old females as above. RNA was immediately extracted and converted to cDNA. RT-PCR was performed with a set of custom designed primers used to detect either membrane (a) or soluble (b) CD137, (n=3 experiments for both (a) and (b)). B2m was used as an endogenous control. (c, d, e, f) ELISA for soluble CD137: CD4^{pos}CD25^{neg}CD137^{neg}, CD4^{pos}CD25^{pos}CD137^{neg} and CD4^{pos}CD25^{pos}CD137^{pos} Tregs from 5–8 week NOD and NOD.B10 *Idd9.3* mice were sorted as above. 50,000 cells were cultured in 96-well U-bottom plate with (c) 25U/ml IL-2 (NOD n=2, NOD.B10 Idd9.3 n=5) or (d) 1.25 ug/ml of anti-CD3 and 25U/ml IL-2 (NOD n=4, NOD.B10 Idd9.3 n=4) for 4 days. ELISA for soluble CD137 was performed on the supernatants. (e) NOD CD4^{pos}CD25^{neg}CD137^{neg}, CD4^{pos}CD25^{pos}CD137^{neg} and CD4^{pos}CD25^{pos}CD137^{pos} T cells

were sorted from 5–7 week old NOD mice as above. 50,000 $CD4^{pos}CD25^{neg}CD137^{neg}$ T cells were plated in U-bottom 96 well plates with 50,000 CD3/CD28 beads and 25,000 (1:2, n=5 experiments) $CD137^{neg}$ or $CD137^{pos}$ Tregs. The supernatant was collected on day 4 and ELISA was performed on the supernatants for soluble CD137. The statistical analysis was performed using the unpaired t test. (f) 20–37 week old non-diabetic NOD (n=6) and NOD.B10 *Idd9.3* (n=7) were sacrificed and their serum tested for soluble CD137 by ELISA. Statistical analysis was performed using the unpaired t test.